5
Solid state spectroscopy II: XAFS and PES

BL5U

Angle-resolved Photoemission Study of $CeCoGe_{1.2}Si_{0.8}$ in the Three-dimensional Momentum Space

H.J. Im[1,2], T. Ito[2,3], S. Kimura[2,3], J.B. Hong[1], Y.S. Kwon[1]

[1]*BK21 Physics Research Division and Institute of Basic Science, Sungkyunkwan University, Suwon 440-746, Korea*

[2]*UVSOR Facility, Institute for Molecular Science, Okazaki 444-8585, Japan*

[3]*School of Physical Sciences, The Graduate University for Advanced Studies, Okazaki 444-8585, Japan*

Recently, $CeTX_2$ systems (T = transition metals, X = semiconducting elements) have intensively studied because of several intriguing phenomena such as heavy fermion behavior with J = 5/2 in $CeCoGe_2$ [1], valence fluctuation in $CeNiSi_2$ [2], and strongly anisotropic magnetic and transport properties in $CeNiGe_2$ [3]. Hybridization of localized *f*-electrons with conduction electrons (*f-d* hybridization) plays an important role to derive the above properties. In order to understand these interesting physical properties, it is important to clarify the electronic structure of this system. Therefore, we have performed the angle-resolved photoemission spectroscopy (ARPES) on $CeCoGe_{1.2}Si_{0.8}$ with large *f-d* hybridization strength in the three-dimensional momentum (*k*-) space at BL5U.

Figure 1(a) shows the energy distribution curves (EDCs) measured at T = 10 K and θ = 0° (normal emission) with changing the photon energy ($h\nu$) from 48 to 88 eV. Peak positions represent the band dispersion along the k_y-direction. We can recognize that there are two weakly dispersed bands around E_B = 0.4 and 1.2 eV with the bottom and top at $h\nu$ = 66 eV, respectively. This indicates that $h\nu$ = 66 eV is a symmetry point in the k_y-direction, and is found to correspond to the Γ-point with inner potential, V_0 = 15.8 eV.

Figure 2(a) shows the Fermi surface (FS) in the k_{zx}-k_y plane as depicted by the shaded plane in Fig. 1(b), mapped with the energy window from E_B = 100 to -100 meV. There are two kinds of FS: One is a large FS, which is continuously formed along k_y-direction in the range of from $k_{zx} \approx 0.5$ to 0.7 Å^{-1} as guided by a dashed line. Other FS inside large FS also seems to open along k_y-direction. In comparison to band dispersions around Γ and Y-points as shown in Fig. 2(b) and (c), respectively, the opened large FS consists of bands which cross E_F at around k_{zx} = 0.6 Å^{-1} ,forming hole pockets.

As a result, the large hole FS that opens along the k_y-direction indicates the quasi-two-dimensional electronic structure. This is consistent with the results of transport experiments (large anisotropy of electrical resistivity, $\rho_c/\rho_{ab} \approx 700$ [4]) and suggests that the *f-d* hybridization strength has anisotropy due to two-dimensionality.

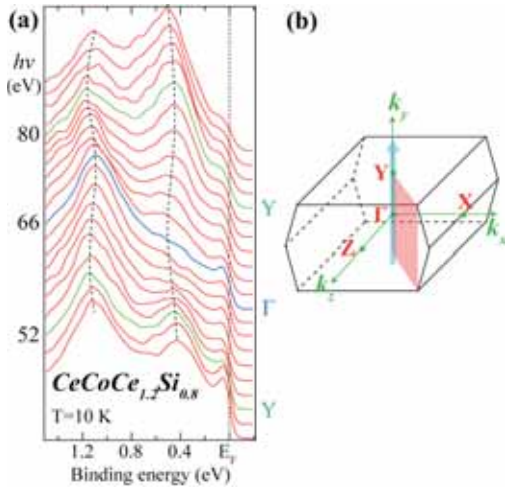

Fig. 1. (a) EDCs of $CeCoGe_{1.75}Si_{1.25}$ observed by $h\nu$-dependent ARPES. The dashed lines are guides to the eye. (b) Brillouin zone of the single-faced orthorhombic structure. The bold arrow and shade plane stand for the measurement path and plane, respectively.

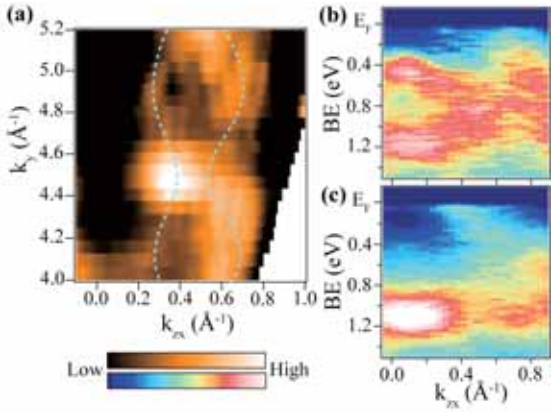

Fig. 2. (a) FS mapping of $CeCoGe_{1.75}Si_{1.25}$ in the k_{zx}-k_y plane as depicted by the shaded plane in Fig 1(b). ARPES intensity plot representing the band dispersions along k_{zx}-direction at around Y- (k_y = 4.89 Å^{-1}, b) and Γ- (k_y = 4.52 Å^{-1}, c) points, respectively.

[1] E.D. Mun *et al*., Phys. Rev. B **69** (2004) 085113.
[2] E.D. Mun *et al*., Phys. Rev. B **67** (2003) 033103.
[3] M.H. Jung *et al*., Phys. Rev. B **66** (2002) 054420.
[4] Y.S. Kwon et al., private communication (2007).

BL1A

Local Structure Analysis of Aluminum Compounds by an XAFS Method

T. Kurisaki[1], Y. Inoue[1], H. Wakita[1,2]

[1]*Department of Chemistry, Faculty of Science, Fukuoka University, Nanakuma, Jonan-ku, Fukuoka 814-0180, Japan*

[2]*Advanced Materials Institute, Fukuoka University, Nanakuma, Jonan-ku, Fukuoka 814-0180, Japan*

Aluminum compounds collected much interest because of their ability to act as catalysts, and functional materials. The function of aluminum compound is concerned closely with that coordination structure. For various aluminum compounds, we have studied the electronic structure by X-ray absorption spectroscopy [1, 2]. This result suggested that there is correlation in the form of XANES spectrum and the local structure

In this work, we applied the x-ray absorption near edge structure (XANES) spectroscopy to aluminum compounds combined with oxygen atoms. The results of the measurement indicate unoccupied and occupied electronic structure of aluminum compounds. The X-ray absorption spectra were measured at BL1A of the UVSOR in the Institute of Molecular Science, Okazaki [2]. The ring energy of the UVSOR storage ring was 750MeV and the stored current was 110-230 mA. Al K-edge absorption spectra were recorded in the regions of 1620-1750eV by use of two KTP(011) crystals. The absorption was monitored by the total electron yield using a photomultiplier. The samples were spread into the carbon tape on the first photodynode made of CuBe of the photomultiplier.

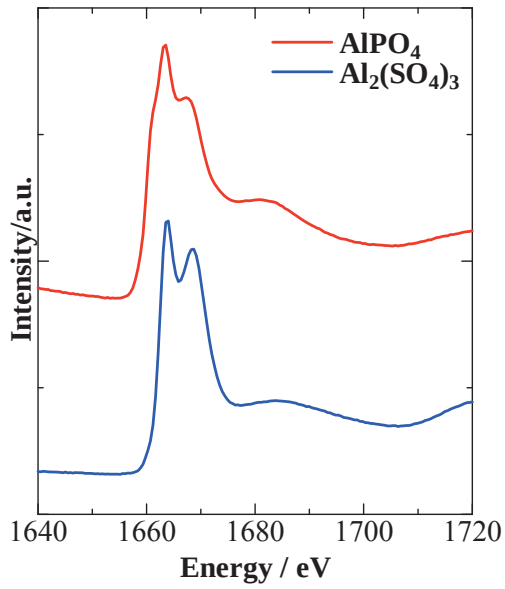

Fig. 1 Observed Al K-edge XANES spectra of aluminum phosphate and aluminum sulfate

The Al K-edge XANES spectra for the aluminum phosphate and aluminum sulfate are shown in Fig. 1. A remarkable change of the spectral patterns was observed for the aluminum phosphate and aluminum sulfate. This result showed that the two aluminum compounds have different electronic state. We are going to try to analyzed this change from comparison of Al K edge XANES and calculated spectra by DV-Xα molecular orbital calculations.

[1] H. Ichihashi, T. Kurisaki, T. Yamaguchi, T. Yokoyama, and H. Wakita, Jpn. J. Appl. Phys. Part 1, **38**(suppl.) (1999) 101.

S. Matsuo, K. Shirouzu, Y. Tateishi and H. Wakita, Adv. Quan. Chem. **42** (2002) 407.

[3] S. Murata, T. Matsukawa, S. Naoè, T. Horigome, O. Matsuodo, and M. Watatabe, Rev. Sci. Instrum. **63** (1992) 1309.

BL1A

Characterization of Aluminum Naphthalocyanine Complexes by an XAFS Method

T. Kurisaki[1], Y. Inoue[1], H. Wakita[1,2]

[1]*Department of Chemistry, Faculty of Science, Fukuoka University, Nanakuma, Jonan-ku, Fukuoka 814-0180, Japan*

[2]*Advanced Materials Institute, Fukuoka University, Nanakuma, Jonan-ku, Fukuoka 814-0180, Japan*

Phtalocyanines (PC) and their derivatives are of particular interest due to many possible applications, such as catalyst, medical supply, semiconductor, and high sensitivity colorimetric regent. Naphthalocyanine (NPC) has a largely p-conjugated. In order to elucidate the effect of the axial ligand, it is necessary to determine their electronic structure [1]. But the electronic structure of naphthalocyanine is not well known.

In this work, we applied the x-ray absorption near edge structure (XANES) spectroscopy to analyze the structure of AlNPC-Cl. The results of the measurement indicate unoccupied and occupied electronic structure of AlNPC-Cl complex. The X-ray absorption spectra were measured at BL1A of the UVSOR in the Institute of Molecular Science, Okazaki [2]. The ring energy of the UVSOR storage ring was 750MeV and the stored current was 110-230 mA. Cl K-edge absorption spectra were recorded in the regions of 3000-3285eV by use of two InSb(111) crystals. The absorption was monitored by the total electron yield using a photomultiplier.

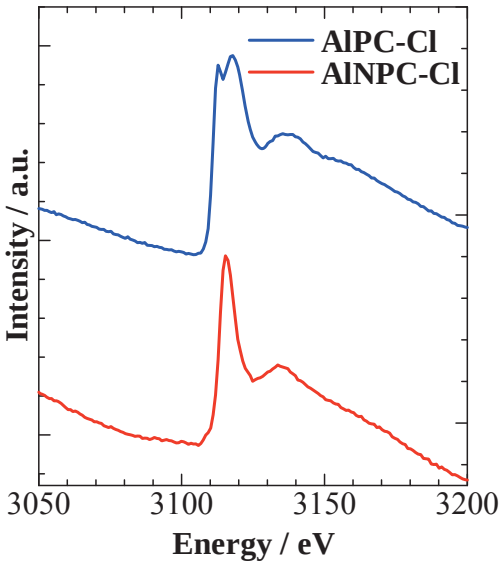

Fig. 1 Observed Cl K-edge XANES spectra of AlNPC-Cl and AlPC-Cl

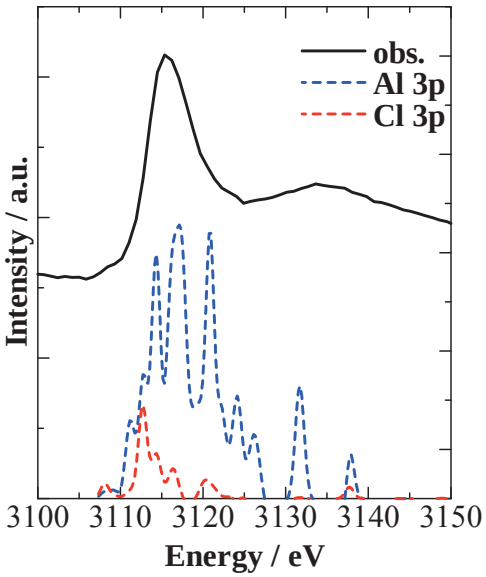

Fig. 2 Observed and calculated Cl K-edge XANES spectra of AlNPC-Cl.

The Cl K-edge XANES spectra for AlNPC-Cl and AlPC-Cl are shown in Figs. 1. A remarkable change of the spectral patterns was observed for AlNPC-Cl and AlPC-Cl. The observed and calculated Cl K XANES spectra for AlNPC-Cl are shown in Fig. 2. Comparison of observed and calculated spectra revealed that aluminum 3p and chloride 3p orbits contribute to the first peak. However, AlNPC-Cl did not contain the contribution from the N 2p and Al 3d orbits.

[1] J. Simon F. Tournilhaec and J. –J. André, Nouv. J. Chim. **10** (1986) 295.

[2] S. Murata, T. Matsukawa, S. Naoè, T. Horigome, O. Matsuodo, and M. Watatabe, Rev. Sci. Instrum. **63**, (1992) 1309.

BL1A

Study of Local Structure of Al-*K* Edge for Modified Hydrotalcite (Layered Double Hydroxide)

A. Nakahira[1], H. Murase[1], H. Nagata[1], S. Nakamura[1], T. Kubo[1], H. Aritani[2]
[1]*Faculty of Engineering, Osaka Prefecture University, Gakuencho, Sakai 599-8531, Japan*
[2]*Saitama Institute of Technology, Fukaya 369-0293, Japan*

Introduction

Layered double hydroxide (LDH) is a clay mineral with a layered structure, in which its composition formula is $[M(II)_{1-x}\ M(III)_x(OH)_2]^{x+}\cdot[A^{n-}_{x/n}\cdot YH_2O]$. M(II), M(III) and exchangeable anions in LDH are able to substitute to various cations and anions. In the present study, we focus on the structure evaluation of basic LDH composed of Mg^{2+} and Al^{3+}, which is called hydrotalcite, MgAl-LDH. Furthermore, it is known that various mixed oxide was generated by calcination of LDH. Obtained mixed oxide is expected to be applicable to many fields such as adsorption and ion exchange materials, magnetic materials, catalysis, and environmental purification materials since it has high specific surface area and unique rehydration behaviors. However, it is not clarified about he structure evaluation of basic LDH and the detailed structure of mixed oxides generated of LDH from 300 to 500°C.

In the present study, the structure evaluation of basic LDH composed of Mg^{2+} and Al^{3+}, which is called hydrotalcite, and mixed oxide obtained by calcination of MgAl-LDH at 300 to 500°C were performed.

Experiments

Mixing solution was adjusted by mixing 0.2 mol/dm^3 $MgCl_2$ aqueous solution and 0.1 mol/dm^3 $AlCl_3$ aqueous solution. MgAl-LDH with M^{2+}/M^{3+} =2 were synthesized by adding mixing solution into 0.05 mol/dm^3 $NaHCO_3$ at room temperature. 1 mol/dm^3 NaOH was simultaneously added into the aqueous solution in order to keep pH 10. After precipitation was finished, products for MgAl-LDH were aged at room temperature for 2 hours. They were separated from liquid phase and sufficiently washed by deionized water and finally air-dried at 110°C for 24 hours.

Mixed oxides were obtained by calcination at 200, 300, 400, and 500°C for 2 hours of MgAl-LDH. The local structures around Al were characterized by measuring X-ray adsorption near edge structure (XANES) at BL1A in UVSOR with KTP.

Results and Discussion

Products prepared by co-precipitation method identified to be layered double hydroxide consisted of Mg^{2+} and Al^{3+} by powder X-ray diffraction analysis. Then, it was suggested that mixed oxide generated by calcination of obtained MgAl-LDH had broad peaks derived from rock salt structure from XRD results.

Figure 1 shows the results of XANES of Al-*K* edge of some mixed oxides. All were different from oxides like α and γ-Al_2O_3 and a hydroxide like $Al(OH)_3$. The spectrum of mixed oxide obtained at 200°C corresponded approximately to that of MgAl-LDH. It was elucidated that Al-K edge XANES spectra of mixed oxides generated at 300, 400, and 500°C was similar to that of MgAl-LDH, although peaks was broad with temperature.

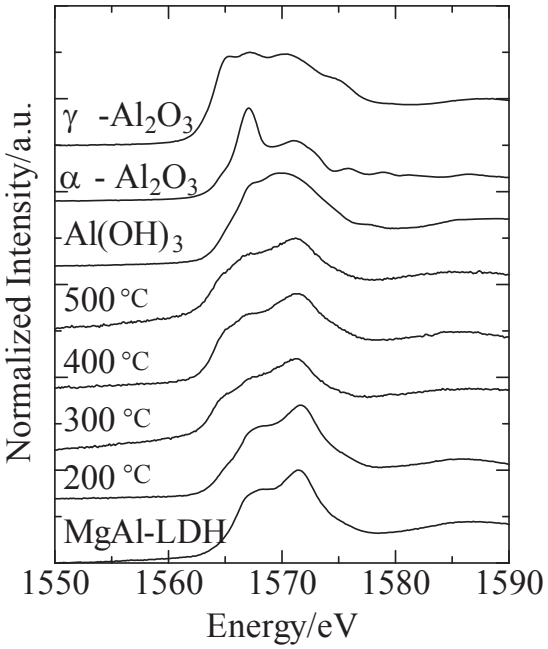

Fig. 1 Al-*K* XANES of MgAl-LDH products and samples obtained by calcination of MgAl-LDH at various temperatures. α-Al_2O_3 and γ-Al_2O_3 are reference materials.

BL1A

Study of Si K-edge of Local Structure in Mesoporous Silica Bulk Prepared by Hydrothermal Hot-pressing

A. Nakahira[1], H. Nagata[1], M. Takimura[2], S. Nakamura[1], T. Kubo[1], H. Aritani[3]
[1]*Faculty of Engineering, Osaka Prefecture University, Gakuencho, Sakai 599-8531, Japan*
[2]*Faculty of Engineering, Kyoto Institute of Tech, Matsugasaki, Kyoto 605-8585, Japan*
[3]*Saitama Institute of Technology, Fukaya 369-0293, Japan*

Mesoporous silica MCM-41 have attracted much attention because of their possible uses as supports for catalysts, a host for nanosize materials and adsorption. However, since bulks of mesoporous structure could not be obtained by conventional solidified methods such as sintering, the application of mesoporous materials is limited. Nakahira et al reported that densified bulky MCM-41 was successfully synthesized using hydrothermal hot-pressing (HHP) method [1]. Therefore, we attemped to exmine the local structure around Si of MCM-41 bulk by XANES spectra.

MCM-41 powder was prepared as a starting material [2]. Mixture of powder and water was heated at 150°C with uniaxial pressing under 40MPa and kept constant for 2 hours. Obtained bulks were identified by XRD. Si K-edge XANES spectra were obtained in a total electron yield mode at room temperature using a KTP double–crystal monochrometer at BL01A of the UVSOR. The spectra were collected in the photon energy range from 1700 to 1925 eV atintervals of 0.05 eV with a dwell time of 1 s.

XRD results showed that MCM-41 bulk was also retained the mesopores after HHP. Figure 1 shows the results of Si K-edge XANES of MCM-41 bulk and starting material powder ((a) and (b)). Silicagel (c) was used as a reference material of amorphous silica with coordiation number 4. The spectrum of HHP bulk was significantly similar to those of starting powder and silicagel. Hence, there is no apparent change in the relative intensity nor the width of these spectra. These results of XANES spectra revealed that the local structure around Si enviroment was almost unchanged before or after HHP treatment.

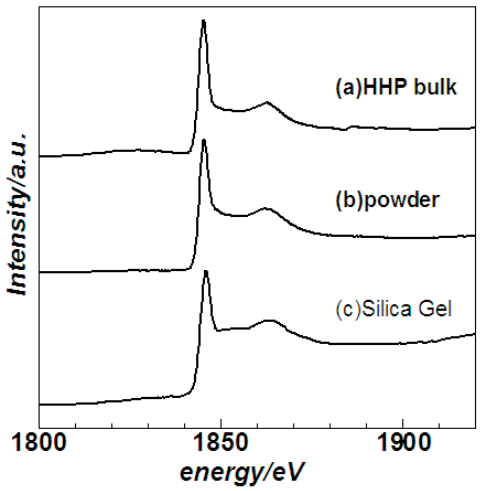

Fig. 1 Si K-edge XANES spectra of MCM-41 bulk prepared by HHP.

[1] H. Nagata, M. Takimura, Y. Yamasaki and A. Nakahira, Materials Transactions, **47** (08) (2006) 2103-2105
[2] H. P. Lin and C. Y. Mou, Science, **273** (1996) 765-768.

BL1A

Measurement of X-ray Excited Optical Luminescence from a Silica Glass

T. Yoshida[1], T. Tanabe[2], H. Yoshida[3]
[1]*Department of Materials, Physics and Energy Engineering, Nagoya University, Furo-cho, Chikusa-ku, Nagoya 464-8603*
[2]*Department of Advanced Energy Engineering Science, Interdisciplinary Graduate School of Engineering Science,Kyushu University6-10-1, Hakozaki, Higashi-ku, Fukuoka 812-8581*
[3]*EcoTopia Science Institute, Nagoya University, Furo-cho, Chikusa-ku, Nagoya 464-8603*

Introduction

Radiation effects on silica glasses are one of the main concerns for their application as optical windows, insulators and optical fibers under fusion and fission environments. Although the radiation damage of silica glass has been extensively studied, the detailed damaging processes and/or radiation effects are not yet fully understood.

In the present study, we have utilized soft X-ray as a radiation source. Since the energy region of the soft X-ray covers the *K*- and *L*-edges of silicon and oxygen, it enables us to study the effects of preferential excitations of inner-shell electrons on the defect production and/or annihilation. We thus examined the changes in X-ray excited optical luminescence (XEOL) of a silica glass with respect to excitation X-ray energy near the threshold of the Si *K*-edge, irradiation time and temperature.

Experimental

The sample used in this study was a low-OH fused silica glass (T-2030) disc produced by Toshiba Ceramics, Japan. The diameter and thickness of the sample were 13 mm and 2 mm, respectively. XEOL of the silica glass by X-ray energy between 1.8 and 1.9 keV was measured between 50 K and 300 K on the beam line 1A at UVSOR-II, Institute for Molecular Science. The luminescence was collected and guided by a lens in a UHV chamber to the monochromator (CP-200, JOBIN YVON) and detected by a multi-channel analyser (OMAIII, EG&G PRINCETON APPLIED RESEARCH), which covers the photon energies from ca. 1.5 eV to 4 eV.

Results and Discussion

We selected three excitation X-ray energies of 1834 eV (just below the Si *K*-edge), 1848 eV (on the white line) and 1858 eV (well above the threshold). Fig. 1(a) shows observed XEOL spectra from the sample excited by the three different energies, measured at room temperature. An intense emission band peaked around 3.1 eV is observed in each spectrum. The previous studies assigned the origin of the 3.1 eV band to the intrinsic $B_{2\beta}$ center [1,2]. We reported previously that in-reactor or UV irradiation on silica glasses induced similar emission bands, and this emission band can be induced also by the soft X-ray irradiation, presumably by exciting the electrons trapped at the oxygen-deficient sites.

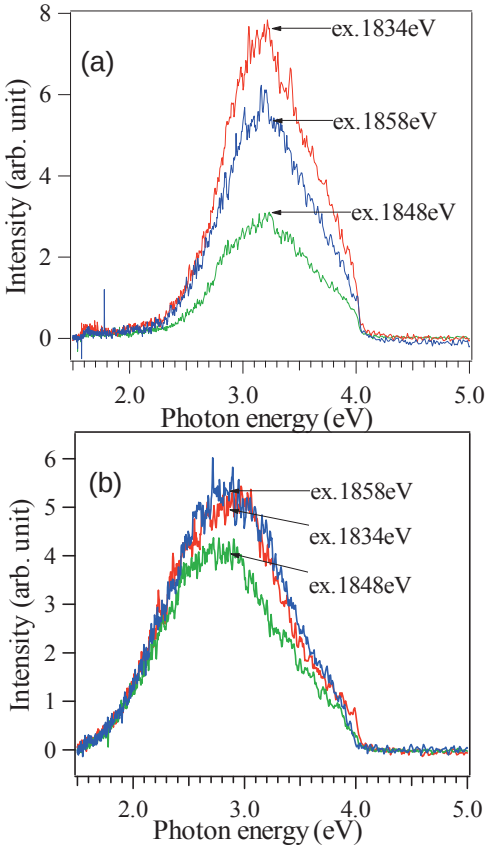

Fig. 1 Optical luminescence spectra of a fused silica glass excited by X-rays with the energies of 1834, 1848 and 1858 eV at (a) 300 K and (b) 50K. Solid curves are two Gaussians peaked at 2.6 and 3.1 eV, resulting from the peak fit for the profile at 1848 eV.

We also measured XEOL at lower temperatures, and found the broadening of the emission band below 100 K. Fig. 2(b) shows XEOL of the same sample measured at 50 K. A peak position is shifted to the lower energy side, because an additional emission band appears around 2.6 eV, revealed by the peak fit, as shown in Fig.2 (b). This additional emission band occurs, presumably because the excited electrons survive longer at lower temperatures until relaxed to the corresponding energy level(s).

[1] R. Tohmon, H. Mizuno, Y. Ohki, K. Sasagane, K. Nagasawa, Y. Hama, Phys. Rev. B **55** (1989) 1337.
[2] S. Agnello, R. Boscaino, M. Cannas, F. M. Gelardi, J. Non-cryst. Solids **232-234** (1998) 323.

BL1A

Atomic Structure of Supersaturated ZnO-Al_2O_3 Solid Solutions

I. Tanaka, S. Yoshioka, F. Oba, T. Yamamoto
Department of Materials Science and Engineering, Kyoto University, Kyoto 606-8501, Japan

X-ray absorption near-edge structure (XANES) is known to be a powerful tool to probe local electronic structure because of its sensitivity to change in chemical environment. It allows us to access the local structure of dopants, utilizing the element selectivity. In the present study, we investigate the local structure of Al solute atoms in ZnO by XANES. Samples are supersaturated solid solution synthesized by pulsed laser deposition (PLD) technique. First-principles calculations are systematically made to evaluate the local atomic structures and energetics. Theoretical XANES is also obtained by first-principles calculations to interpret the experimental spectra.

Experimental and Computational Procedures

Thin film samples were prepared by PLD technique using an excimer KrF* laser source (λ= 248 nm, τ = 25 ns, Lambda physik COMPex205). Laser frequency was kept at 10 Hz. The ceramic samples were used for targets of PLD. Laser power was approximately 3×10^4 J/m^2. All PLD experiments were made in oxygen backfill pressure of p_{O2}=0.3Pa. High purity SiO_2 glass plates were used as substrates. Substrate temperature was 600 ºC. High-resolution X-ray absorption spectra at the Al K-edge were measured using the BL1A beamline at UVSOR. The XANES spectra were collected by the total electron yield (TEY) method. The incident photon beam was monochromatized using a KTP ($2d_{011}$=10.954Å) double-crystal monochromator. Samples were mounted using adhesive carbon tapes. No surface coating to avoid charging was found to be necessary.

In order to reproduce XANES by theoretical calculations, it is necessary to take into account the correlation between the core-hole and the excited electron. [1] It can be evaluated in a straightforward way using all-electron methods. Therefore, first-principles all-electron calculations based on orthogonalized linear combination of atomic orbitals (OLCAO) method [2] were employed in the present study. Theoretical XANES spectra were obtained within the electronic-dipole transitions. The core-hole effects were fully taken into account by removing one electron on Al 1*s* orbital and putting one additional electron at the bottom of the conduction band. In order to avoid the artificial interactions among core-holes, supercells composed of more than 100 atoms were chosen on the basis of test calculations. Transition energies were obtained as the difference in total energy between the ground and core-hole states. More details of the XANES calculation and its application to dopant characterization can be found elsewhere. [1, 3]

Results and Discussion

X-ray diffraction (XRD) analysis found that ZnO:Al films with Al concentration of less than 19 cation% are composed of a single crystalline phase. It can be assigned as a wurtzite phase with an abnormal expansion in lattice constant *c* by 1.5%. Experimental and calculated XANES are shown in Fig 1. The spectral features of experimental thin film sample are different from those of the reference compound, $ZnAl_2O_4$ having spinel structure. The spectrum is closer to the theoretical spectrum for Al_{Zn} model where Al is located at the substitutional Zn site of wurtzite ZnO. However, this model is found to be inconsistent to the XRD results revealing lattice expansion in the *c* direction. Systematic evaluation of theoretical lattice constants and XANES spectra for models with miscoordinated Al indicates that partial contribution of such Al can provide a consistent explanation of the structural and spectral features.

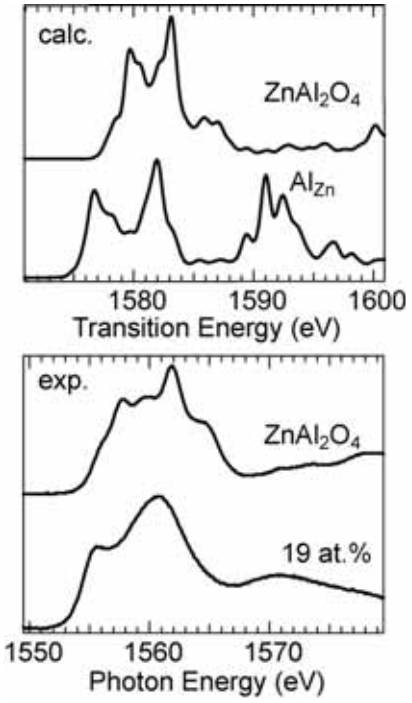

Fig. 1. Theoretical and experimental Al K-edge XANES spectra for $ZnAl_2O_4$ and Al-doped ZnO.

[1] I. Tanaka, T. Mizoguchi, and T. Yamamoto, J. Am. Ceram. Soc. **88** (2005) 2013.
[2] W. Y. Ching, J. Am. Ceram. Soc. **73**, 3135 (1990).
[3] I. Tanaka *et al.*, Nature Mater. **2** (2003) 541.

BL1A

Structural Analysis of Active Mo species on H-MFI for Methane Dehydroaromatization with Hydrogen

H. Aritani[1], N. Naijo[1], K. Takanashi[1], H. Orihara[1], A. Nakahira[2]
[1]*Faculty of Engineering, Saitama Institute of Technology, Fukaya 369-0293, Japan*
[2]*Graduate School of Engineering, Osaka Prefecture Universitty, Sakai 599-8531, Japan*

Supported Mo catalysts on H-MFI zeolites show noted high and selective activity to convert methane to benzene. Because the catalytic process, so-called "GTL (Gas to Liquid)" one, is conventional and quite selective for liquefaction of natural gases, catalysts with high and durable activity have been called for. However, design of the catalysts with durable activity for methane dehydroaromatization is very difficult because of carbon deposition and/or grafting during the reaction. For MoO_3/H-MFI, Mo species are reduced to form several types of carbide species (Mo^{2+} mainly) in the initial reaction step (at above 973 K), and the carbide species play a role for methane activation to form CH_x intermediates. At the same time, H_2 is outgassed. On H-MFI support, oligomerization of CHx intermediates assist to form benzene. Selectivity of benzene formation is based on the sieving by microporous structure of H-MFI. Therefore, relation between the H-MFI support (with surface acidity) and active Mo species formed in the reaction is thus important to clarify the formation process and its stability of highly active Mo.[1,2] In this study, Mo L_{III}-edge XANES is applied to characterize the Mo species on H-MFI with various SiO_2/Al_2O_3 ratios.

All the catalysts were prepared by impregnation of each silica-alumina support with ammonium heptamolybdate solution (7.5wt% loading as MoO_3), and followed by drying and calcination at 773 K for 3 h. H-MFI (Si/Al_2=40, 72, 90, and 1880) supports were synthesized hydrothermally at 443 K for 7 days, and followed by ion-exchange (NH_4^+) treatment and calcination at 773 K. Mo L_{III}-edge XANES spectra were measured in BL1A of UVSOR-IMS in total-electron yield mode at ambient temperature.

For evaluation of catalytic activitty for methane dehydroaromatization at 973 K, it is concluded that MoO_3/H-MFI(Si/Al_2=40) in low Mo contents (2.5-5.0 wt% as MoO_3) shows the maximun benzene yield in an initial streaming range. In this case, deactivation due to carbon deposition can not be avoided. It is definitely that rate of deactivation becomes low by coexistence of H_2 (CH_4/H_2=20) in the reaction. Figure 1 shows the L_{III}-edge XANES spectra of MoO_3(5.0wt%)/H-MFI(Si/Al_2=40) catalysts after methane dehydroaromatization with/without H_2. Second derivatives of XANES spectra are also shown in Fig. 2. After the reaction with CH_4 (denoted as [A]), Mo_2C-like species are formed, indicating a reduction and carbinding of Mo ions. Because of partially oxidized (due to coexistence of Mo^{4+} or others), spectral feature is slightly different from that of Mo_2C. [2] It indicates that highly active Mo species are consist of Mo2C (in major) and partially oxidized species such as oxycarbide species. After the reaction with CH_4+H_2 (denoted as [B]), the spectrum is quite similar to that of CH_4 reaction. Thus H_2 coexistence brings about depression of coaking but be independent on reduction of active Mo species. In case of H2 reduced catalysts in a pretreatment, the spectrum (denoted as [C]) is quite similar to bare Mo_2C. In this case, low dehydroaromatization activity is shown. It is concluded that excess reduction enhance the formation of Mo2C species, and low activity is brought about at the same time.

[1] H. Aritani et al., UVSOR Activity Report, **33**, (2006) 92.
[2] H. Aritani et al., Chem. Lett. **35** (2006) 416.

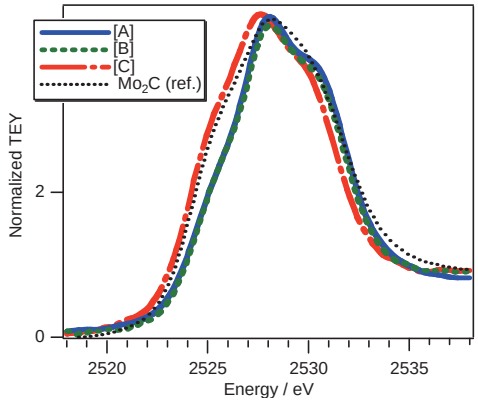

Fig.1 Mo L_{III}-edge XANES of 5wt% MoO_3/H-MFI (Si/Al_2=40). [A] After reaction with CH_4(20%)+He.; [B] After reaction with CH_4(20%)-H_2(1%)-He.; [C] After pretreatment with H_2 and reaction with CH_4 (20%)-H_2(1%)-He.

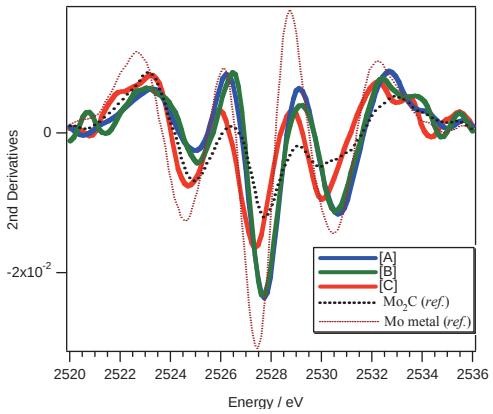

Fig. 2 Mo L_{III}-edge XANES of 5wt% MoO_3/H-MFI (Si/Al_2=40). [A] After reaction with CH_4(20%)+He.; [B] After reaction with CH_4(20%)-H_2(1%)-He.; [C] After pretreatment with H_2 and reaction with CH_4(20%)-H_2(1%)-He.

Unoccupied Electronic States of Inner Organic Thin Films: Soft X-ray Absorption Spectra of Pentacene Derivative Films

H.S. Kato[1], R. Hirakawa[1,2], F. Yamauchi[1,2], M. Kawai[1,2], T. Hatsui[3], N. Kosugi[3]
[1]*RIKEN (The Institute of Physical and Chemical Research), Wako 351-0198 Japan*
[2]*Dept. of Advanced Materials Science, Univ. of Tokyo, Kashiwa 277-8651 Japan*
[3]*Dept. of Vacuum UV photoscience, Institute for Molecular Science, Okazaki 444-8585 Japan*

Introduction

In order to extend new functionality of electronic devices, the molecular devices have recently been investigated with great efforts. In most of the devices, the properties of organic molecules are controlled by the applied electric field and charge injection. The organic field effect transistor (OFET) is the typical molecular device that controls of electric conductivity by injection of carriers into the organic thin film under the applied electric field. Based on the knowledge of inorganic semiconductor transistors, the conductive mechanism has generally been understood with a scheme of band bending of electronic states. However, the energy diagram may not be the same between inorganic and organic materials, because of more localized orbitals of the organic molecules. It is also important to elucidate the difference of electronic states for using the noble characters of organic molecular materials for the future advanced devices. Therefore, the direct observation of electronic state changes in the organic thin films under the applied electric field has been required.

In this study, we aim to establish a new experimental method that elucidates the electronic state change in organic molecular thin-films under the electric field, using model OFET devices. In general, X-ray absorption spectroscopy (XAS) is measured by the detection of Auger electrons emitted after X-ray absorption. However, the mean free path of the electrons, typically less than 1 nm, in bulk is too short for detection of the electronic states of inner organic thin films, of which typical thickness is about 100 nm. Thus, we attempted the fluorescence yield detection for XAS.

Experimental

The XAS measurements were carried out at BL4B and BL3U of UVSOR facility in IMS. We fabricated 6,13-dihydrodiazapentacene thin films on the SiO_2-covered Si substrates using a deposition system in RIKEN. Then, the samples were set in the measurement chamber at BL3U through ambient conditions. The typical base pressure at the XAS measurements was less than 10^{-5} Pa. Both the Auger electron yield and the fluorescence yield were observed using a retarding-field detector equipped with MCP plates.

Results and Discussion

The N K-edge XA spectra of the same 6,13-hydrodiazapentacene film (t = 100 nm) on SiO_2-covered Si substrate by detecting both the Auger electron yield and the fluorescence yield, as shown in Figs. 1(a) and 1(b), respectively. In both measurements, the photon energies of each component are almost the same, while the relative intensities are different.

One of the obvious differences is the detection of a peak at 398 eV. The intense peak is characteristic in the Auger electron yield spectra that are surface sensitive. Since its relative intensity increased with increasing time of ambient gas exposure, the origin of the peak would be an attachment of any impurities or surface oxidation. Thus, we concluded that the fluorescence yield spectra show the intrinsic electronic state of 6,13-dihydrodiazapentacene, which has also been supported by a molecular orbital calculation of the isolate molecule. In the fluorescence spectra, the observed π^* and σ^* peaks have clear incidence angle dependence. These evidence a good oriented structure of the molecules in the inner thin film, as the pentacene thin films on flat substrates.

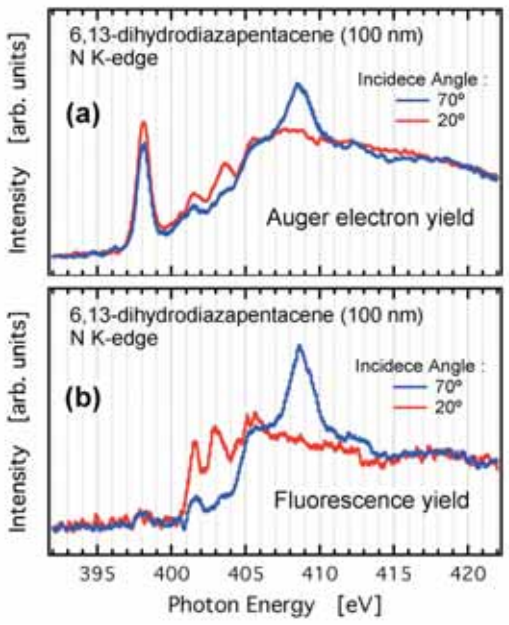

Fig. 1. N K-edge XA spectra of a 6,13-dihydrodiazapentacene film (t = 100 nm) on SiO_2-covered Si substrate: (a) Auger electron yield spectra, (b) fluorescence yield spectra. In both measurements, incidence angle dependence was performed at 70° and 20° from the surface normal, and then the intensity of the spectra was normalized by a height at around 420 eV in photon energy.

BL4B

Study on the Surface and Bulk Structures of the Positive Electrode for Li-Ion Battery Cells with High Power-Type

H. Kobayashi, M. Shikano

Research Institute for Ubiquitous Energy Devices, AIST, Ikeda, Osaka, 563-8577 Japan

Several of the requirements of rechargeable batteries for hybrid electric vehicles (HEVs) are quite different to those of portable electronic devices. In particular, high specific power and long calendar life are very important requirements of HEV applications. Much effort has been applied to understanding the mechanisms that limit the calendar life of high power Li-ion cells. Until now, although the deterioration in the performance of currently available lithium batteries is thought to result from problems with the positive electrodes, the mechanism of deterioration of the electrodes is still poorly understood. Detailed information on the changes taking place in both the cathode and anode on cycling is essential in order to determine the origin of the degradation of performance. In this study, $LiNi_{0.8}Co_{0.2}O_2$-based positive electrodes from cells that had undergone power fading through cycling tests were examined by XANES analysis to obtain information on their surfaces. The relationship between power fade and the surface state of the positive electrode will be studied.

Experimental

We used cylindrical battery cells of capacity 400 mAh for this study, which were designed to have a rate capability of more than 10 C. The positive and negative electrode was comprised of $LiNi_{0.8}Co_{0.2}O_2$ -based oxides and hard carbon, respectively. Each cell was characterized using the standard battery test procedure given in PNGV Battery Test Manual. The change in DC resistance was checked every few cycles. After completion of the degradation test, the SOC of the cell was adjusted to 0% immediately before disassembling it, since the chemical and physical properties of the active materials are influenced by the SOC. After disassembly of the SOC-adjusted cell, the surface of the positive electrode was examined by XANES in order to study the surface film or phase transitions in particles of the active material. The O K-edge XANES spectra of the samples were measured on the BL4B beamlines of the UVSOR Facility. Data were obtained in the total electron yield (TEY) and fluorescence yield (FY) modes.

Results

Figure 1 shows the cycle dependence of the DC resistance. DC resistance increased from 1.08 to 1.74 on increasing the test temperature from 20 ºC to 80 ºC. Above 80 ºC, an abrupt increase in DC resistance was observed. Figure 2 shows the O K-edge XANES spectra of 0% SOC samples before and after test. In TEY mode, O K-edge XANES spectra provide information on the surface structure. The spectrum measured before cycle testing contained peak A, corresponding to oxygen originating from the layered structure, and peaks B and C. After the cycle tests, the intensity of peak A clearly decreased at 80 ºC, while the intensities of peaks B and C showed no significant changes. The position of peak B was close to that of the NiO spectrum, indicating the existence of a cubic phase on the surface, and the position of peak C was close to that of Li_2CO_3, or to conductive materials such as AB (data not shown). When measured in FY mode, O K-edge XANES spectra provide information on the bulk structure. Here, essentially the same spectra were observed before and after the cycle tests for both samples. The strong peak A originating from the layered structure of the positive electrode was observed in FY mode. However, peak B was absent and peak C was much lower in intensity. These results indicate that the surface structure is different to that of the bulk in this system. Furthermore, it is clear that part of the layered structure at the surface of the $LiNi_{0.8}Co_{0.2}O_2$ -based positive electrode was transformed to a cubic structure at 80 ºC, although the layered structure was retained in the bulk.

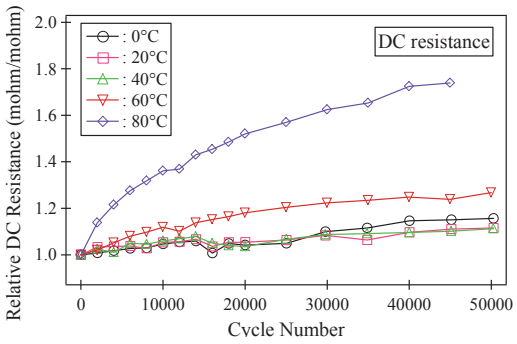

Fig.1 Cycle dependence of retention of DC resistance.

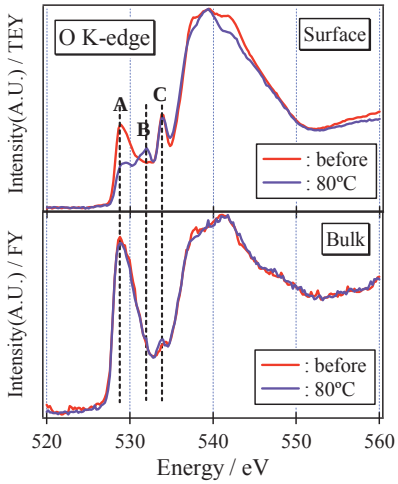

Fig.2 O K-edge XANES spectra for the positive electorrode after 45000 cycle test at 80 ºC.

BL5U

Core-Level Photoemission Study of Alkyl-Passivated Si Nanoparticles

A. Tanaka[1,2,3], T. Kamikake[2], K. Tomio[1], N. Takashima[4], M. Imamura[3], Y. Murase[2]
[1]*Department of Mechanical Engineering, Faculty of Engineering, Kobe University, Kobe 657-8501, Japan*
[2]*Department of Mechanical Engineering, Graduate School of Science and Technology, Kobe University, Kobe 657-8501, Japan*
[3]*Department of Mechanical and Systems Engineering, Graduate School of Science and Technology, Kobe University, Kobe 657-8501, Japan*
[4]*Department of Physics, Faculty of Science and Engineering, Konan University, Kobe 658-8501, Japan*

Introduction

Recently, the various Si nanostructures have a great interest, since it has been reported that they show a strong visible photoluminescence and a possibility of future integrating electronic devices with optical sensing technique is suggested. However, the interplay to their optical properties between the intrinsic quantum confinement effects and extrinsic surface/interface properties is still controversial. In order to understand the intrinsic properties of Si nanostructures, it is indispensable to characterize their surface chemical properties. In this work, we have carried out the core-level photoemission studies of alkyl-passivated Si nanoparticles synthesized by the solution routes in order to characterize their surface electronic structures.

Experiment

Synthesis procedure of *n*-butyl-passivated Si nanoparticles used in this work is described elsewhere [1]. Core-level photoemission measurements were performed at BL-5U of UVSOR II Facility.

Results and Discussion

Figure 1 shows the Si 2*p* core-level photoemission spectrum of *n*-butyl-passivated Si nanoparticle with mean diameter of 1.4 nm. As shown in Fig. 1, it is found that the present Si 2*p* core-level spectrum is reproduced by two components fairly well. From the analogy with the previous results of alkyl-terminated bulk-Si(111) surfaces [2], the lower- and higher-binding-energy features originate from the inner Si atoms of Si nanoparticles (bulk component) and surface Si atoms of Si nanoparticles bonded to surface-passivants of *n*-butyl groups (surface component), respectively. As shown in Fig. 1, this surface component accompanies with the chemical shifts to higher binding energies relative to the bulk components. This indicates the different chemical states in the surface Si atoms bonded to *n*-butyl groups with the inner Si atoms and existence of a chemical reaction (chemisorption) between the surface-passivants of *n*-butyl groups and Si nanoparticles. It has been reported in the previous work [2] that the chemical shifts for surface Si atoms of methyl- (CH_3-), pentyl- (C_5H_{11}-), and decyl- ($C_{10}H_{21}$-) terminated bulk-Si(111) surface are 0.27, 0.21, and 0.21 eV, respectively. On the other hand, the chemical shift of *n*-butyl-bonded Si atoms of the present Si nanoparticles is 0.33 eV. An important point to note is that the chemical shift of the surface component in the present Si nanoparticle is significantly larger than those of surface components of alkyl-terminated bulk Si surfaces. This indicates that the interfacial features between the surface Si atoms and surface passivants of alkyl groups, and therefore the bonding natures between the surface-passivants of alkyl groups and surface Si atoms, such as a coordination number and configuration of surface-passivants, are different among the bulk Si surface and Si nanoparticle surface.

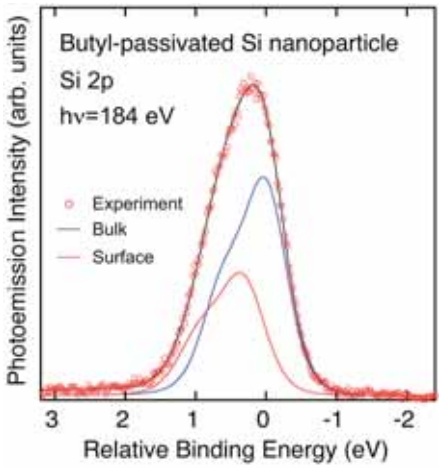

Fig. 1. Si 2*p* core-level photoemission spectrum of *n*-butyl-passivated Si nanoparticle with mean diameter of 1.4 nm measured with $h\nu$=184 eV. Result of line-shape analysis is also shown. Observed spectrum is decomposed into bulk component (blue line) and surface component bonded to surface *n*-butyl molecules (red line).

[1] A. Tanaka *et al*., Solid State Commun. **140** (2006) 400.
[2] J. Terry *et al*., J. Appl. Phys. **85** (1999) 213.

BL5U(FEL)

Threshold Photoemission Magnetic Circular Dichroism using Free Electron Laser

T. Nakagawa, T. Yokoyama, M. Hosaka, M. Katoh
Department of Electronic Structure, Institute for Molecular Science, Okazaki 444-8585 Japan
UVSOR Facility, Institute for Molecular Science, Okazaki 444-8585 Japan

Introduction

Magnetic circular dichroism (MCD) in the x-ray regions (XMCD) has widespread over the synchrotron radiation facilities because of its high sensitivity to the element specific magnetism. On the other hand, MCD in the regions from infrared to ultraviolet (UV) is also a useful tool for the study of ferromagnetic ultrathin films. The magneto-optical Kerr effect (MOKE) detects the rotation and distortion of the polarization of reflected lights from magnetic materials. The Kerr effect in valence bands in thin films usually rotates the polarization and changes the ellipticity only by 10^{-2}-10^{-6}rad. In the valence band photoemission, nevertheless, extensive works have been performed using circularly polarized synchrotron radiation and angle-resolved measurement, showing high (~30%) asymmetry. [1,2]

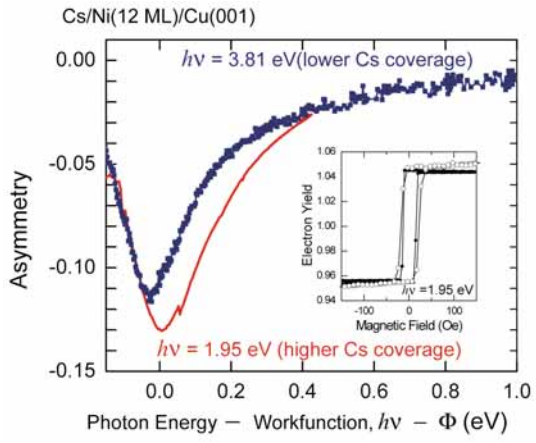

Fig. 1 MCD asymmetry as a function of maximum kinetic energy(photon energy–work fuction) on perpendicularly magnetized Ni(12ML)/Cu(001). The photon energies used are 1.95 eV and 3.81 eV. The inset shows magnetization hysteresis curves by MCD and MOKE measurements, which are identical to each other.

We have investigated the observation of enhanced MCD near the Fermi level using visible and ultraviolet lasers in a total yield mode. [3] More than 10% MCD asymmetry is achieved on perpendicularly magnetized 12 ML Ni film on Cu(001), and magnetization curves are obtained. By changing the work function with the aid of cesium adsorption, the laser experiments show that the MCD asymmetry is enhanced only near the photoemission threshold, and that the asymmetry drops to 0.1% for photon energy larger than the work function by 0.6 eV. A theoretical calculation also shows enhanced dichroism near the photoemission threshold, in agreement with the experimental result.

To obtain the high MCD asymmetry we have to tune the photon energy a little higher than the workfunction. We have used tunable free electron laser from UVSOR-II, which can deliver lower energy than $h\nu$ = 6.3 eV, close to typical workfunction for transition metal surfaces without surface modification such as alkali metal adsorption. Thus FEL at UVSOR-II is a suitable source to threshold photoemission MCD measurements. Fig. 2 shows a magnetization hysteresis curve on Ni(8 ML)/Cu(001) using $h\nu$ = 5.37 eV, where the photoemission threshold for Ni is ~5.3 eV. As is expected from the result shown in Fig. 1, the asymmetry is high, ~6%. This result clearly evidences that the clean Ni surface also shows high asymmetry near the photoemission threshold.

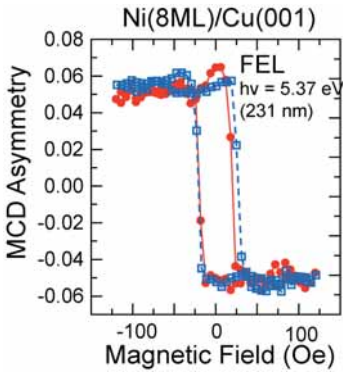

Fig. 2 Magnetization hysteresis curves on a clean eight monolayer Ni film grown on Cu(001) obtained by FEL-MCD and MOKE. The photon energy of FEL is 5.37 eV.

[1] C. M. Schneider, *et al*., Phys. Rev. B **44** (1991) R12066.
[2] W. Kuch and C.M. Schneider, Rep. Prog. Phys. **64**(2001) 147.
[3] T. Nakagawa, and T. Yokoyama, Phys. Rev. Lett. **96**(2006) 237402.
[4] T. Nakagawa, T. Yokoyama, M. Hosaka, and M. Katoh, Rev. Sci. Instrum. **78** (2007) 023907.

Adsorpiton of Benzene on Au(111) Surface by Angle-Resolved Ultravoilet Photoemission Spectroscopy

L. Wang[1], D. Qi[1], A. T. S. Wee[1], T. Mochizuki[2], H. Miyazaki[2], T. Ito[3], S. Kimura[3], J. Yuhara[2], K. Soda[2]

[1]*Department of Physics, National University of Singapore, Singapore 117542*
[2]*Graduate School of Engineering, Nagoya University, Nagoya 464-8603 Japan*
[3]*UVSOR Facility, Institute for Molecular Science, Okazaki 444-8585 Japan*

Introduction

Molecules have been shown to operate as Coulomb blockade structures, diodes, switching devices with high negative differential resistance (NRD) and conductance switches, making the nascent field of molecular electronics very promising[1]. The central issue in molecular electronics is the characteristics of the molecule-metal interface which strongly influences the transport properties in the molecular device[2]. Benzene/Au system is chosen as testbed since benzene is a typical molecule with delocalized π orbitals and gold is one of the most widely used substrate. In this study, the adsorption of benzene on Au(111) surface have been investigated by angle-resolved photoemission spectroscopy.

Experimental

Au(111) surfaces were prepared by cycles of Ar^+ ion bombardment at 1 KeV and annealing at 800 K in an ultrahigh vacuum system. The (1x1) reconstruction was clearly observed on clean Au (111) surface by low energy electron diffraction. Benzene (99%, company name) was *in situ* evaporated onto Au(111) surface which was cooled down to 5 K. One monolayer of benenze on Au was achieved by introducing the dosage of 1 Lagmuir assuming the stick coefficient =1. Angle-resolved photoelectron spectra were recorded under 2.7×10^{-8} Pa with a high-resolution energy analyzer at BL5U. The total energy resolution was 14 meV with the excitation photon energy of 29.3 eV at 5 K.

Results and Discussion

Figures 1 show the photoemission intensity of surface state on clean Au(111) along $[\bar{1}10]$ direction. A dispersion near the Fermi edge with the maximum binding energy of 430 meV at Γ point can be clearly observed, which is consistent with that for Shockley-type surface state on Au(111) [3].

Figure 2 shows the angle-integrated valence band spectra for benzene mononlayer adsorbed on Au(111) at the various temperatures. After the adsorption, some noticeable features, which are originated from benzene molecules[4], emerge in the binding energy range from 8-14 eV. On the other hand, the Shockley-type surface state of Au(111) is immediately extinguished, indicating the presence of a strong interaction between the benzene molecules and the gold surface. This interaction can not be described only as purely physical interaction.

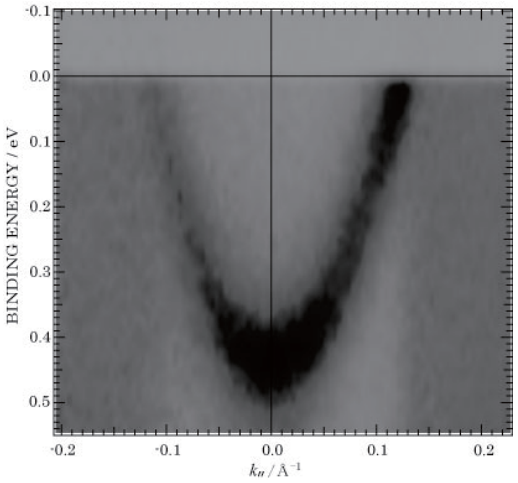

Fig.1 Photoemission intensity of Schockely-type surface state on clean Au(111) along $[\bar{1}10]$ direction as a gray scale.

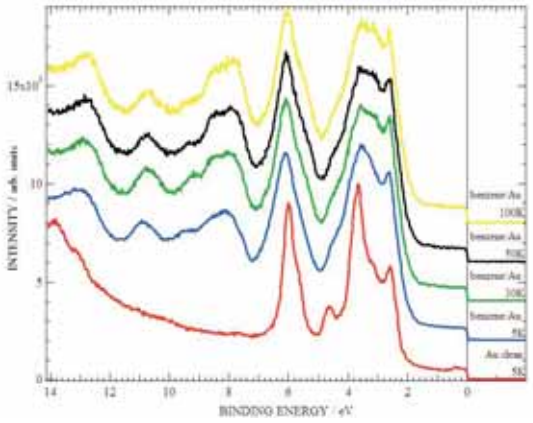

Fig.2 Angle-integrated valence band spectra for clean Au(111) and benzene/Au(111) at various temperatures.

[1] M. A. Reed *et al*., Science **278** (1997) 252; Z. J. Donhauser *et al*., Science **292** (2001) 2303.
[2] J. G. Kushmerick *et al*., Phys. Rev. Lett. **89** (2002) 086802; L. Wang *et al.*, J. Am Chem. Soc. **128** (2006) 8003.
[3] S. D. Kevan *et al*., Phys. Rev. B **36** (1987) 5809; R. Paniago *et al.*, Surf. Sci. **336** (1995) 113.
[4] Y. K. Kim *et al.,* Phys. Rev. B **71** (2005) 115311.

BL5U

Electronic Structure and Stability of the Pd-Ni-P Bulk Metallic Glass

T. Takeuchi[1], D. Fukamaki[2], H. Miyazaki[3], K. Soda[3]
T. Itoh[4], S. Kimura[4]

[1]*EcoTopia Science Institute, Nagoya University, Nagoya 464-8603 Japan*
[2]*Department of Applied Physics, Nagoya University, Nagoya 464-8603 Japan*
[3]*Department of Quantum Mechanics, Nagoya University, Nagoya 464-8603 Japan*
[4] *Institute for Molecular Science, Okazaki 444-8585 Japan*

Bulk metallic glasses (BMGs) have attracted a great deal of interests because of their ability in practical usage, such as mechanical parts of high strength, surface coating materials with high degree of hardness, soft-magnetic materials, etc. In order to design the BMGs suited for each practical usage, stabilization mechanism of the BMG's has to be revealed from microscopic viewpoints; the local atomic arrangements and the electronic structure. Since it is naturally considered that the highly-stable BMGs possess a low free-energy, the stabilization mechanism of BMG's should be discussed in terms of free-energy, which is mostly determined by the electronic structure.

We investigate, in this study, the electronic structure of the Pd-Ni-P BMG, that is one of the most famous, stable BMGs obtained in metal-metalloid systems, by employing the relevant crystals with the first principle cluster calculation, band calculation, and high-resolution photoemission spectroscopy. By calculating electronic structure of the relevant crystals, in which the structure units of the BMG (trigonal prism clusters with a phosphorus atom in the center) are formed, we found that the these units (trigonal prism clusters) possess covalent nature and highly stable. The formation of the covalent bonds in the clusters (relevant crystals) was further confirmed by observations of the bonding bands in the high-resolution photoemission spectra.

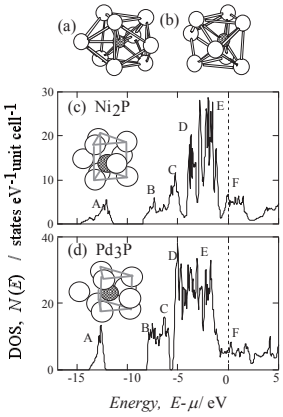

Figure 1 (a)Trigonal prism cluster and (b)tetragonal dodecahedron cluster (deformed trigonal cluster) exist in the Pd-Ni-P bulk metallic glass. Electronic density of states of the relevant crystals, (c) Ni2P, and (d) Pd3P calculated by the FLAPW-GGA method (Wien2K). The density of states of the relevant crystals are commonly characterized by possession of the narrow bands marked as A - F. The bands A-C are bonding bands, while the corresponding anti-bonding bands exist far above E_F. The bands D and E are nearly non-bonding d-bands. These configurations provide a strong covalent nature.

We also calculated the cluster-orbitals of large clusters consisting of two trigonal clusters with different inter-cluster-connections, and found that the electronic structure does not significantly altered by the inter-cluster connection with keeping the bonding-bands far below the Fermi level. This characteristic leads to flexible connections of the clusters. The trigonal clusters, therefore, are able to construct a random network to form the bulk metallic glass without significantly increasing their internal energy. The enhanced entropy and the small internal energy result in the very low free-energy of the BMG.

We conclude, therefore, that the Pd-Ni-P BMG is stable because of the random cluster network of the rigid, stable, large structure unit (cluster) of covalent nature. This stabilization mechanism is applicable for the Zr-based BMG's and even for the silica glasses, and, therefore, commonly acceptable for highly-stable amorphous solids.

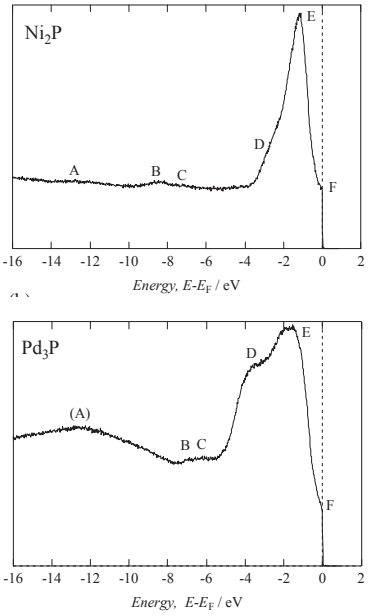

Figure 2 High-resolution photoemission spectra of the (a)Ni2P and (b)Pd3P measured with an incident energy of 40eV. The characteristics of electronic structure expected from band-calculation and cluster-calculation are qualitatively reproduced in the spectra.

BL5U

Electronic Structure of Pd-Ni-P Bulk Metallic Glass

S. Ota[1,2], T. Suzuki[1], H. Miyazaki[1,2], K. Soda[1,2], T. Takeuchi[3],
M. Hasegawa[4], N. Nishiyama[5], H. Sato[6], U. Mizutani[7], T. Ito[2], S. Kimura[2]
[1]*Graduate School of Engineering, Nagoya University, Nagoya 464-8603 Japan*
[2]*Institute for Molecular Science, Okazaki 444-8585 Japan*
[3]*EcoTopia Science Institute, Nagoya University, Nagoya 464-8603 Japan*
[4]*Institute for Materials Research, Tohoku University, Sendai 980-8577 Japan*
[5]*R&D Institute of Metals and Composites for Future Industries, Sendai 980-8577 Japan*
[6]*Aichi University of Education, Kariya 448-8542 Japan*
[7]*Toyota Physical and Chemical Research Institute, Nagakute-cho, Aichi-gun 480-1192 Japan*

Introduction

Bulk metallic glasses (BMG) possess excellent mechanical, physical and chemical properties, which come from their amorphous structure. In spite of their thermodynamical metastability, Pd-based BMG have large glass forming ability (GFA) [1]. In order to understand the mechanism of their large GFA, we have studied the electronic structure of $Pd_xNi_{80-x}P_{20}$ BMG by photoemission spectroscopy (PES) and theoretical calculation for local clusters expected in BMG.

Experimental

The PES measurement was carried out at 25 K under 2×10^{-8} Pa. $Pd_xNi_{80-x}P_{20}$ specimens were prepared by a casting method and their clean surfaces were obtained by *in situ* scraping with a file.

The theoretical calculation was performed by the DV-$X\alpha$ method with a code SCAT [2] for a Pd_3Ni_6P cluster in a form of a capped trigonal prism, which is derived from a crystalline $PdNi_2P$ [3].

Results and Discussion

Valence-band spectra of $Pd_xNi_{80-x}P_{20}$ recorded at excitation photon energies $h\nu$ are shown in Fig.1. They were normalized by the integrated intensity up to the binding energy E_B of 10 eV. There are three bands at $E_B \sim 0.8$, 2.2, and 3.9 eV, which are ascribed to the Ni 3*d*-, Pd 4*d*-, and Pd 4*d*-derived states, respectively, judging from the $h\nu$-dependence of their photoionization cross sections [4]. The spectral shape for $x = 45$ is not so much different from one for $x = 40$, while the Ni 3*d* band is relatively large for $x = 35$. There is almost no peak shifts for these bands.

In Fig.2, a spectrum recorded at $h\nu = 40$ eV is compared with the density of states calculated for the cluster in the inset, where a black sphere represents P at the center, green and blue ones for Pd at corners of the prism and a top of the cap, and yellow and pink ones for Ni at the corners and the tops, respectively. Taking account of the difference in photoionization cross sections [4], both results agree very well with each other. This suggests that the cluster may be a dominant form in $Pd_{40}Ni_{40}P_{20}$. The calculation also shows a strong P-(Pd, Ni) bonding. In the Pd-Ni-P BMG, the network of such clusters may be formed by sharing their vertices and sides with large flexibility in the inter-cluster bond direction, as in the silica glass.

[1] A. Inoue, Acta Mater. **48** (2000) 279.
[2] H. Adachi *et al*., J. Phys. Soc. Jpn. **45** (1978) 875.
[3] M.Vennstrom *et al*., J. Sol. Stat. Chem. **177** (2004) 1449.
[4] J. J. Yeh and I. Lindau, Atom. Data and Nucl. Data Tables **32** (1985) 1.

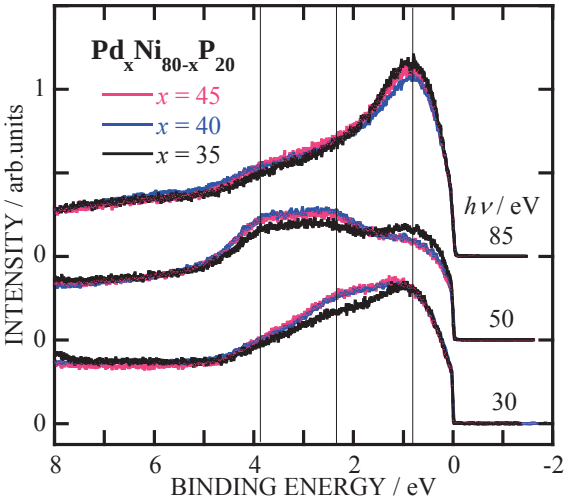

Fig.1 Valence-band spectra of $Pd_xNi_{80-x}P_{20}$.

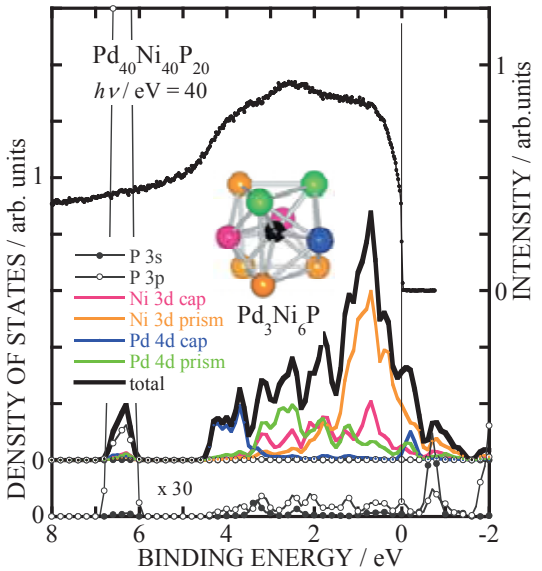

Fig.2 Valence-band spectrum of $Pd_{40}Ni_{40}P_{20}$ and calculated density of states for Pd_3Ni_6P cluster.

Electronic Structure of $(Fe_{1-x}Re_x)_2VAl$ and $Fe_2(V_{1-y}Ti_y)Al$

K. Yamamoto[1], H. Miyazaki[2,3], T. Mochizuki[2], T. Suzuki[2], S. Ota[2]
M. Kato[2], S. Yagi[2], Y. Nishino[4], K. Soda[2,3]
[1]*School of Engineering, Nagoya University, Nagoya 464-8603 Japan*
[2]*Graduate School of Engineering, Nagoya University, Nagoya 464-8603 Japan*
[3]*Institute for Molecular Science, Okazaki 444-8585 Japan*
[4]*Graduate School of Engineering, Nagoya Institute of Technology, Nagoya 466-8555 Japan*

Introduction

Heusler-type Fe_2VAl and its related alloys have attracted much attention because Fe_2VAl shows remarkable enhancement of thermoelectric power on partial substitution by the forth element [1]. In this paper, we will report results on the Fe and V 3*p*-3*d* resonance photoemission study of *p*-type alloys $(Fe_{1-x}Re_x)_2VAl$ and $Fe_2(V_{1-y}Ti_y)Al$ in order to clarify the relation between changes in their thermoelectric properties and electronic structure on the substitution.

Experimental

Photoelectron spectra were recorded at 20 K under 1.8 x 10^{-8} Pa. The origin of the binding energy E_B, the Fermi level E_F, and total energy resolution were determined by measuring the Fermi edge of a gold film. The total energy resolution was 63 meV at the photoexcitation energy $h\nu$ = 80 eV. Specimens used in this study were polycrystalline alloys of Fe_2VAl, $(Fe_{1-x}Re_x)_2VAl$ and $Fe_2(V_{1-y}Ti_y)Al$. Clean surfaces for the measurement were prepared by *in situ* fracturing the specimens.

Results and Discussion

Figure 1 shows typical valence band spectra recorded at $h\nu$ = 80 eV together with a bulk-sensitive one of Fe_2VAl at $h\nu$ = 900 eV [2]. In Fe_2VAl, there are a shoulder structure A near E_F and four bands B, C, D and E at E_B = 0.4, 0.8, 1.6 and 3.0 eV, respectively. The overall features agree well with those in theoretical density of states [3] and the bulk-sensitive spectrum except for the feature around E_F: the large intensity of the shoulder A observed in this study is attributed to surface states appearing in a pseudogap across E_F in the bulk electronic structure. On the partial substitution of Ti or Re, the shoulder A becomes indistinct with increase in the intensity at E_F and the valence band shifts to the low binding energy side as a whole, as expected in a rigid band model. This rigid-band-like shift results in the enhancement of their thermoelectric power.

Partial densities of Fe and V 3*d* states of Fe_2VAl and $(Fe_{0.95}Re_{0.05})_2VAl$, which were estimated by the 3*p*-3*d* resonance photoemission, are compared in Fig. 2 together with their valence-band spectra. By the Re substitution, the V 3*d*-derived band D shifts to the low binding energy side due to the interaction with the Re 5*d* states, while the Fe and V 3*d*-derived band C shows no shift and the intensity near E_F is relatively increased by the Fe 3*d* states: the band width of the Fe 3*d* states seems to be extended by the interaction between the Re 5*d* and Fe 3*d* states.

[1] Y. Nishino, The Science of Complex Alloy Phases (Ed. by T. B. Massalski and P. E. Turchi, TMS, Warrendale, 2005) p.325.
[2] K. Soda *et al.*, Phys. Rev. B **71** (2005) 245112.
[3] G. Y. Guo *et al.*, J. Phys.: Condens. Matter. **10** (1998) L 119.

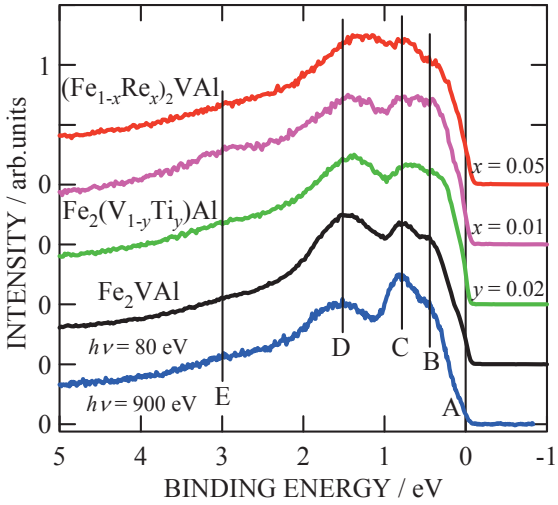

Fig.1 Valence band photoelectron spectra.

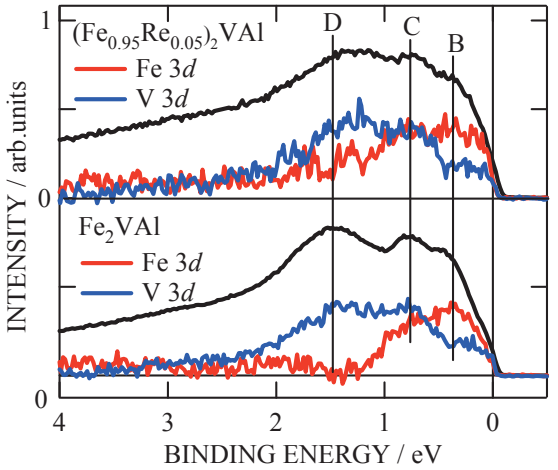

Fig.2 Partial densities of Fe 3*d* and V 3*d* states in Fe_2VAl and $(Fe_{0.95}Re_{0.05})_2VAl$.

Electronic Structure and Glass Forming Ability of Zr-Cu-Al Bulk Metallic Glasses

T. Suzuki[1], H. Miyazaki[1,2], S. Ota[1,2], M. Inukai[1], M. Kato[1], S. Yagi[1], K. Soda[1,2]
H. Kato[3], M. Hasegawa[3], T. Takeuchi[4], H. Sato[5], U. Mizutani[6], T. Ito[2], S. Kimura[2]
[1]*Graduate School of Engineering, Nagoya University, Nagoya 464-8603 Japan*
[2]*UVSOR, Institute for Molecular Science, Okazaki 444-8585 Japan*
[3]*Institute for Materials Research, Tohoku University, Sendai 980-8577 Japan*
[4]*EcoTopia Science Institute, Nagoya University, Nagoya 464-8603 Japan*
[5]*Aichi University of Education, Kariya 448-8542 Japan*
[6]*Toyota Physical and Chemical Research Institute, Nagakute-cho, Aichi-gun 480-1192 Japan*

Introduction

Bulk metallic glasses (BMG's) possess the large glass forming ability (GFA) and show physical, chemical and mechanical properties, which are superior to crystalline materials [1]. In order to understand the origin of their large GFA from the microscopic point of view, we have systematically studied electronic structure of Zr-Cu-Al BMG's using photoelectron spectroscopy.

Experimental

Photoelectron spectra were recorded under 2 x 10^{-8} Pa at 25 K at BL5U. Total energy resolution and the origin of the binding energy E_B, *i.e.* the Fermi level E_F, were determined by the Fermi edge of an evaporated Au film.

Specimens were ternary Zr-Cu-Al BMG's in a size of ϕ 1~2 mm x 3 mm. These compositions are shown in Fig.1 by symbols A ~ H with a counter map of their reduced glass temperatures T_g/T_l (T_g: glass transition temperature, T_l: liquidus temperature), which is regarded as one of parameters representing GFA. Clean surfaces for the photoelectron measurement were prepared by *in situ* scraping the specimen with a diamond file.

Results and Discussions

Figure 2 shows typical Zr 4*d* spectra of Zr-Cu-Al recorded at the excitation photon energy of 40.5 eV. These spectra are normalized with their Cu and Zr compositions so that the spectral intensity may be proportional to the density of occupied Zr 4*d* states per Zr atom. Arrows indicate peak positions of the Zr 4d bands. There is a tendency recognized that the peak binding energy and integrated intensity of the Zr 4*d* bands are increased with the Zr composition increasing from H to A. This may suggest the increase in the covalent interaction around Zr atoms with increasing the Zr composition.

The peak position (●) and integrated intensity (■) of the Zr 4*d* band are plotted as a function of T_g/T_l in Fig.3. As seen in the figure, they decrease as T_g/T_l increases: the covalent nature of Zr is relatively weak for Zr-Cu-Al with the large GFA. According to Nakano *et al.* [2], there are two typical local atomic arrangements appearing in Zr-Cu-Al: the Zr-centered covalent cluster and the Cu- or Al-centered metallic clusters, which have relatively low and high structural degree of freedom, respectively. Thus, the present results suggest that the weakening of the covalent nature of Zr and the increase in the structural degree of freedom may lead to the large GFA.

[1] M. Telford, Mater. Today **7** (2004) 36.
[2] S. Nakano *et al.*, *private communication.*

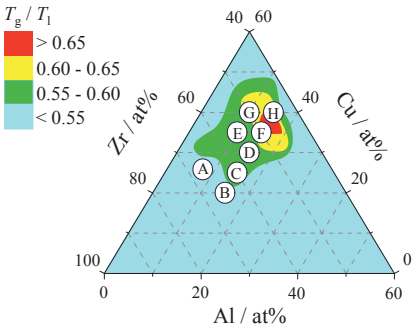

Fig.1 Compositional dependence of T_g/T_l

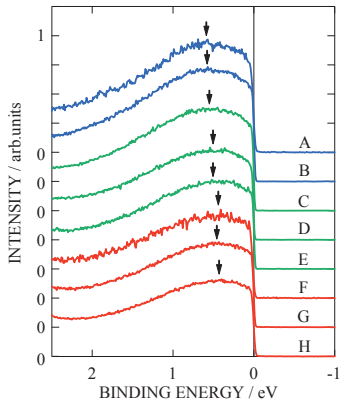

Fig.2 Typical spectra of Zr 4*d* band of Zr-Cu-Al BMG's.

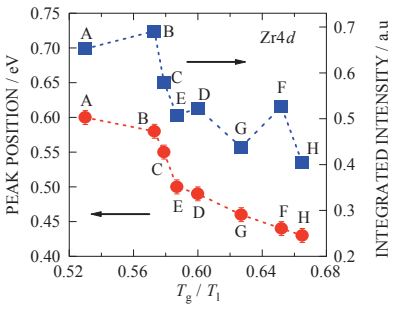

Fig.3 Peak position and integrated intensity of Zr 4*d* band as a function of the reduced glass temperature T_g/T_l.

BL5U

Three-Dimensional Angle-Resolved Photoemission Study on EuO Thin Films

H. Miyazaki[1,2], T. Ito[2,3], S. Ota[1,2], H. J. Im[4], S. Yagi[1], M. Kato[1], K. Soda[1,2], S. Kimura[2,3]

[1]*Graduate School of Engineering, Nagoya University, Nagoya 464-8603, Japan*

[2]*UVSOR Facility, Institute for Molecular Science, Okazaki 444-8585, Japan*

[3]*School of Physical Sciences, The Graduate University for Advanced Studies, Okazaki 444-8585, Japan*

[4]*Department of Physics, Sungkyunkwan University, Suwon 440-746, Korea*

EuO is a ferromagnetic (TC ~ 70 K) semiconductor. In Eu excess case (Eu-rich EuO), it shows a metal insulator transition (MIT) near the TC ~ 150 K [1, 2]. To clarify the origin of MIT and enhancement TC mechanism of Eu-rich EuO from the microscopic electronic structure view, we investigated the fundamental electronic structure of EuO and Eu-rich EuO. In this report, we have performed in situ three-dimensional angle-resolved photoemission spectroscopy (3D-ARPES) on single crystalline EuO thin films.

EuO thin films have been grown by a molecular beam epitaxy (MBE) method. To obtain high-quality single-crystalline films, we evaporated Eu onto BaO buffered Nb-doped SrTiO3 substrates at 350 °C under oxygen pressure of 8 x 10-6 Pa. Epitaxial growth of single-crystal EuO thin films has been confirmed 1 x 1 EuO (100) patterns by LEED and RHEED methods. The sample was transferred to the 3D-ARPES chamber in situ and then the photoemission spectra were measured at UVSOR-II BL5U. Sample temperature was set at 20 K (< TC ~ 70 K).

Figure 1 shows the photon-energy dependence of the ARPES spectra of EuO at normal emission ($k_{//} = 0$ Å^{-1}). Observed spectra mainly show two structure at the binding energy E_B = 1.3 ~ 3.7 eV and 3.7 ~ 8.0 eV. From the comparison with the calculated photo ionization cross section of Eu 4*f* and O 2*p* [3], the lower binding energy side is attributed to Eu 4*f* states and the other is O 2*p* states. Eu 4*f* and O 2*p* bands show small dispersion about 0.2 and 0.3 eV, respectively. Here, we use the dispersion relation

$$(h/2\pi)k_{\perp} = \sqrt{2mE_K \cos^2\theta + V}\ ,$$

where V is the inner potential, E_K is the kinetic energy at the Fermi level E_F and θ = 0 degree. We determined the inner potential V = 13 eV from the symmetry of the dispersive features.

Figure 2 shows the high-resolution ARPES spectra of Eu 4*f* around Γ point (a) recorded at $h\nu$ = 76 eV and X points (b) at $h\nu$ = 38 eV, respectively. Sizable energy dispersion of the Eu 4*f* states is observed at the Γ and X point. The observed dispersive features are the direct evidence for the 3D-lattice effect due to the Eu 4*f* and O 2*p* hybridization. However the dispersion around X point is larger than Γ point. This indicates that the hybridization between Eu 4*f* and O 2*p* states at the X point is stronger. This result is not consistent with the band calculation [4]. The detailed analysis and the further study for temperature dependence ARPES are in progress.

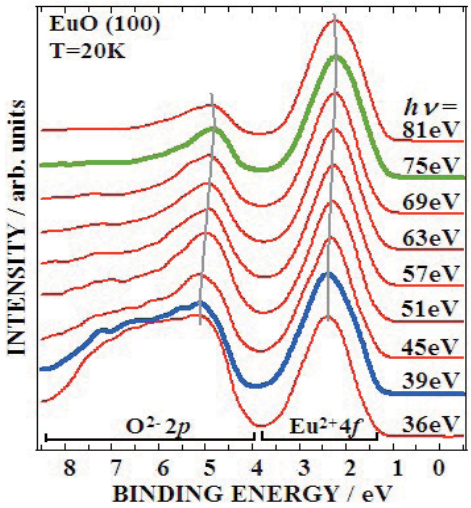

Fig. 1 Photon-energy dependence of the normal emission photoemission spectra of EuO (100).

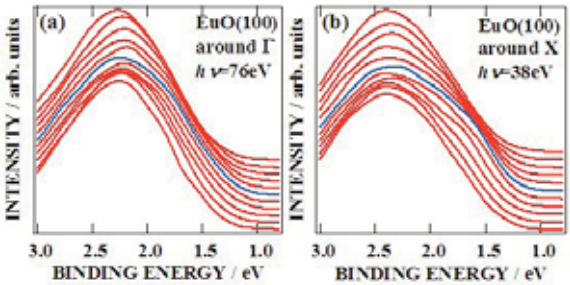

Fig. 2 ARPES spectra of Eu 4*f* around Γ (a) and X (b) points, respectively. The blue lines indicate the spectra at the Γ and X points.

[1] A. Mauger *et al.*,J. Phys. (paris) **39** (1978) 1125..
[2] M. R. Oliver *et al.*, Phys. Rev. B **5** (1972) 1078.
[3] J. J. Yeh and I. Lindau.Atomic Data and Nucl. Data Tables **32** (1985) 1.
[4] S. J. Cho. Phys. Rev. B **1** (1970) 4589.

BL8B1

Characterization of Lithium Compounds by an XAFS Method

T. Kurisaki[1], Y. Inoue[1], H. Wakita[1,2]

[1]*Department of Chemistry, Faculty of Science, Fukuoka University, Nanakuma, Jonan-ku, Fukuoka 814-0180, Japan*

[2]*Advanced Materials Institute, Fukuoka University, Nanakuma, Jonan-ku, Fukuoka 814-0180, Japan*

Lithium compounds are generally used in industrial and commercial applications such as lithium batteries, lithium glasses and other materials. Therefore, it is very interesting to investigate the chemical bonding condition of lithium compounds. However, there are a few reports about Li-K XANES spectra [1].

In this work, we applied the X-ray absorption near edge structure (XANES) spectroscopy to lithium compounds. X-ray absorption spectra of near Li K absorption edges were (XAFS) measured at BL8B1 of the UV-SOR in the Institute of Molecular Science, Okazaki [2]. The energy of the UVSOR storage ring was 750MeV and the stored current was 110-230 mA. The absorption was monitored by the total electron yield using a photomultiplier. We employed the discrete variational (DV)-Xα molecular orbital (MO) method to perform calculated spectra, and compared observed spectra with calculated spectra.

The Li *K* XANES spectra for four lithium halides are shown in Fig. 1. The energy position of each first peak should depend on halide ion. According to the increase in the atomic number of halide ion, the energy of the first peak shifts toward low energies.

The observed and calculated Li K XANES spectra for lithium chloride are shown in Fig. 2. The calculated transition peaks (bars) are convoluted by the Gaussian function of 1.0 eV full width at half maximum (FWHM). The first peak is estimated to the electron transition (mainly Li 1s to unoccupied mixed orbital consisting of Li 2s, Li2p and Cl 3d).

[1] J. Tsuji, K. Kojima, S. Ikeda, H. Nakamatsu, T. Mukoyama and K. Taniguchi, J. Synchrotron Rad. **8** (2001) 554-556

[2] S. Murata, T. Matsukawa, S. Naoè, T. Horigome, O. Matsuodo, and M. Watanabe, Rev. Sci. Instrum. **63** (1992) 1309.

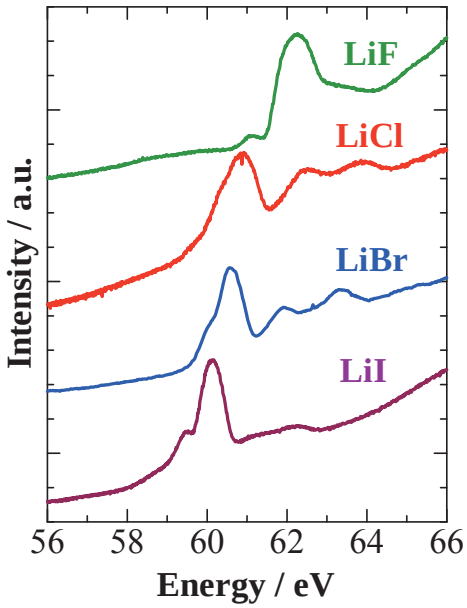

Fig. 1 Li K-edge XANES spectra of lithium halides

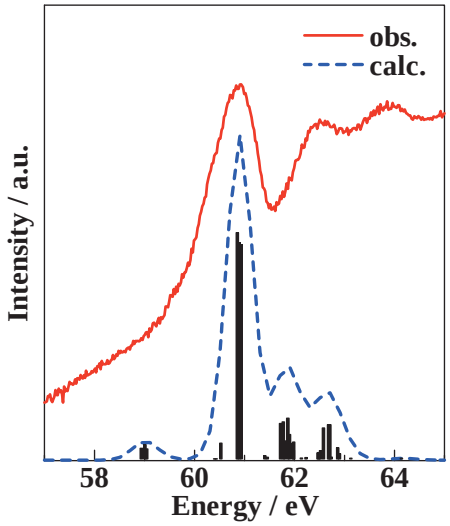

Fig. 2 Calculated transition peaks (vertical bars) and curves (broken line). The solid line is the observed Li K-XANES spectrum for lithium chloride

BL8B1

Comprehensive Classification of DLC Films Formed by Various Methods Using NEXAFS Measurement

A. Saikubo[1], N. Yamada[1], K. Kanda[1], S. Matsui [1], H. Saitoh[2]

[1] Laboratory of Advanced Science and Technology for Industry, University of Hyogo, Kamigori 678-1205 Japan,

[2]Department of Materials Science and Technology, Nagaoka University of Technology, Nagaoka 940-2188, Japan

Introduction

Various diamond like carbon (DLC) thin films have been applied to a large number of industrial fields according to the development of nanotechnology. Recently, classification and standardization of various DLC films are demanded for the expansion of further usage and applications of DLC films. Mechanical, electronic, chemical and optical properties of DLC films are strongly dependent on the elementary composition and the coordination of carbon atoms in films. Near edge X-ray absorption fine structure (NEXAFS) spectroscopy using synchrotron radiation was utilized as an efficient method of sp^2 content for DLC films [1,2]. The sp^2 content can be extracted from the NEXAFS spectrum with a high sensitiveness and a high quantitativeness, because the isolated peak corresponding to the resonance transition from carbon 1s to π* orbital can be observed. In the present study, the 55 kinds of DLC films, which were provided by the enterprises and academic organizations, were discussed by the measurement of NEXAFS spectra.

Experiment

The NEXAFS measurement was performed at the BL8B1 stage of UVSOR in the Institute for Molecular Science. The C K-edge NEXAFS spectra were measured in the energy range 275-320 eV. The energy resolution is estimated to be less than 0.5 eV FWHM. The detection of electrons coming from sample was performed in the total electron yield (TEY) mode. The $sp^2/(sp^2+sp^3)$ ratio in the film can be extracted by normalizing the area of the resonance transition to π* at 285.3 eV with the area of a large section of the spectrum. The absolute $sp^2/(sp^2+sp^3)$ ratio was determined by the comparison with that estimated from the NEXAFS spectrum of graphite. Density of DLC film was measured with X-ray reflectivity method at Nagaoka University of Technology.

Result and Discussion

Determined $sp^2/(sp^2+sp^3)$ ratio populated in the range of 0.1-0.9. Observed samples could be classified roughly to 4 kinds of group by $sp^2/(sp^2+sp^3)$ ratio and density. Group A was characterized by high density, 2.7-3.4 g/cm^3, and low $sp^2/(sp^2+sp^3)$ ratio, ≈0.4. This group consists merely of the sample formed by PVD method. The DLC thin films in this group can be estimated to have high hardness. Group B was characterized by low density, 1.3-2.6 g/cm^3, and high $sp^2/(sp^2+sp^3)$ ratio, 0.8-0.9. This group consists also of the sample formed by PVD method. Group C was characterized by medium density, 1.8-2.4 g/cm^3, and medium $sp^2/(sp^2+sp^3)$ ratio, 0.4-0.6. Most number of samples includes this group and this group consists of samples formed by both PVD and CVD methods. For group A-C, density of DLC film increases with decreasing of $sp^2/(sp^2+sp^3)$ ratio. It is interpreted that the density of DLC film increases with the ratio of sp^3 component in the film. Group D was characterized by low $sp^2/(sp^2+sp^3)$ ratio, 0.2-0.6, in spite of low density, 1.2-2.0 g/cm^3. This group consists almost of the sample formed by CVD method. The peak at ≈288 eV was observed in the several NEXAFS spectra of this group. The presence of this peak indicates the containing hetero-atom, such as nitrogen, and oxygen etc. [3]. These hetero-atoms were considered to reduce π-bonding in the DLC film. Therefore, DLC films with low density were formed in spite of low $sp^2/(sp^2+sp^3)$ ratio.

[1] K. Kanda, T. Kitagawa, Y. Shimizugawa, Y. Haruyama, S. Matsui, M. Terasawa, H. Tsubakino, I. Yamada, T. Gejo and M. Kamada, Jpn. J. Appl. Phys. **41** (2002) 4295.

[2] K. Kanda, Y. Shimizugawa, Y. Haruyama, I. Yamada, S. Matsui, T. Kitagawa, H. Tsubakino and T. Gejo, Nucl. Inst. Meth. B **206** (2003) 880.

[3] K. Kanda, J. Igaki, Y. Kato, R. Kometani and S. Matsui, New Diamond Frontier Carbon Tech. **15** (2005) 123.

BL8B2

The Electronic Structure and the Energy Level Alignment at PTCDA / Metal Interfaces

E. Kawabe[1], H. Yamane[1], K. Koizumi[1], R. Sumii[2], K. Kanai[1], Y. Ouchi[1], K. Seki[1,3]
[1]*Graduate School of Science, Nagoya University, Furo-cho, Chikusa-ku, Nagoya 464-8602 Japan*
[2]*Research Center for Materials Science, Nagoya University,*
[3]*Institute for Advanced Research, Nagoya University*

In recent years, extensive research has been carried out for applying organic materials to electronic devices such as organic light emitting diodes, organic solar cells and organic field effect transistors. It is important to understand how the energy levels align at organic/metal (O/M) interfaces for understanding the mechanism of such devices and for improving their performance, since these factors strongly affect various phenomena such as charge injection. However, the detailed mechanism of the energy level alignment at O/M interface is not yet well understood even for nonpolar molecules. We investigated the electronic structure and the energy level alignment at the interfaces formed by vacuum-depositing perylene -3,4,9,10-tetracarboxylic dianhydride (PTCDA, molecular structure shown in Fig. 2(a)) on polycrystalline vacuum-deposited films of metals (Au, Cu and Co) by ultraviolet photoelectron spectroscopy (UPS).

In the case of PTCDA/Au interface, the apparent interface states or charge transfer (CT) states were not observed in its UPS spectra (not shown here), which indicates that the interaction between Au and PTCDA is very weak, and that PTCDA molecule physically adsorbed on Au surface. The vacuum level (VL) showed sudden shift toward Fermi level (E_F) of Au at the interface, as shown in Fig. 1, indicating the formation of an interface dipole. The possible origins of such interface dipole have been proposed by Ishii *et al.* [1], and we can ascribe the presently observed change at PTCDA/Au interface to the push-back of the electron cloud spilled out from the metal surface (push-back effect) by the adsorption of PTCDA molecules. The interface dipole (Δ) for this lowering of the VL was 0.52 eV.

The UPS spectra at PTCDA/Cu interface are shown in Fig. 2(b). The highest occupied molecular orbital (HOMO) of PTCDA is observed at binding energy (E_B) of 2.47 eV at the film thickness d = 5 nm. At d = 0.4 nm, an additional spectral feature is observed at E_B = 0.2 ~ 1.2 eV. This interface specific structure may be due to the CT from Cu to PTCDA. Actually, the upward VL shift shown in Fig. 1 with Δ = -0.29 eV is consistent with the picture that CT from Cu to PTCDA leading to the rise of VL overwhelmed the push-back effect which tends to lower the VL.

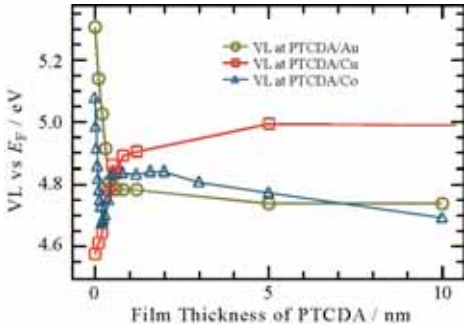

Fig. 1 The film thickness dependence of VL at PTCDA/Au, Cu and Co interfaces.

At PTCDA/Co interface, VL showed upward shift after the initial abrupt downward shift (Fig. 1). Although this upward shift indicates the CT from Co to PTCDA, CT states were not observed in the UPS spectra (Fig. 2(c)), possibly because the amount of the transferred charge is too small to appear as a new state in the spectra. The estimated amount of transferred charge at PTCDA/Cu and PTCDA/Co interfaces by the electrostatic theory [2] for explaining the VL shift are one electron per about two and five PTCDA molecules, respectively.

The schematic energy diagrams of these interfaces are summarized in ref. [3]. We found an interesting behavior at PTCDA/Co interface, so we focus attention on the effect of the d electrons on the energy level alignment.

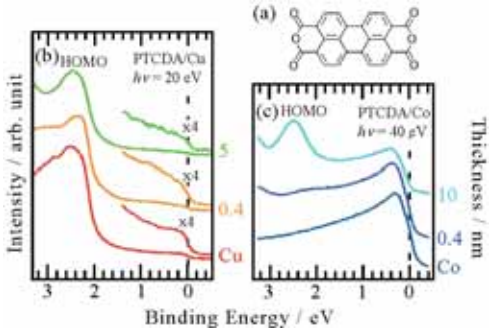

Fig. 2 (a) The molecular structure of PTCDA. (b) and (c) The UPS spectra of PTCDA/Au and PTCDA/Co interfaces, respectively.

[1] H. Ishii, K. Sugiyama, E. Ito and K. Seki, *Adv. Mater.* **11** (1999) 605.
[2] H. Ishii, N. Hayashi, E. Ito, Y. Washizu, K. Sugi, Y. Kimura, M. Niwano, Y. Ouchi and K. Seki, Phys. Stat. Sol. (a) **201** (2004) 1075.
[3] E. Kawabe, H. Yamane, K. Koizumi, R. Sumii, K. Kanai, Y. Ouchi and K. Seki, Mater. Res. Soc. Symp. Proc. **965** (2006) S09-28.

BL8B2

Photoelectron Angular Distribution of 3d-orbital Derived Bands in Mn-Phthalocyanine Monolayer

S. Kera[1], H. Fukagawa[1], T. Kataoka[1], T. Hanatani[1],
R. Sumii[2], S. Nagamatsu[1], N. Ueno[1]
[1]*Graduate School of Science and Technology, Chiba University, Chiba 263-8522 Japan*[#]
[2]*IMS and Graduate School of Science, Nagoya University*
Furo-cho, Chikusa-ku, Nagoya 464-8602, Japan

Angle-resolved ultraviolet photoelectron spectroscopy (ARUPS) has been known as a powerful technique to obtain crucial information on electronic band structure for various kinds of materials. Moreover, for organic thin films, information on the geometrical structure of the thin films can be also discussed in accordance with a quantitative analysis of the ARUPS intensity using photoelectron scattering theory. However, it is noteworthy that the experimental results are still limited to describe the relationships between the distribution of the molecular orbital (MO) and the ARUPS intensity due to a lack of a standard/simple theoretical model and well-ordered organic thin films [1].

We measured the take-off angle (θ) dependences of 2p- and 3d-orbital derived bands in ARUPS spectra for well-ordered Mn-phthalocyanine (Pc) monolayers to clarify the MO distribution affecting to the angular distribution.

Experiments

ARUPS spectra were measured at photon incidence angle $\alpha=45^{o}$, photon energy (hν) of 20 eV and 28 eV, and at a sample temperature T=295 K. The purified MnPc molecules were carefully evaporated onto the graphite (HOPG:ZYA) substrate.

Results and Discussion

Figure 1(a) shows the θ dependence of ARUPS of annealed-MnPc monolayer (0.3nm) on HOPG. The intensity is normalized to the incidence photon flux (I_R). A lowest lying feature appeared at 0.65 eV, where the binding energy is observed lower than previous metal-Pc monolayers on HOPG [2], could be ascribed to HOMO band of MnPc. The next feature at 1.2 eV is assigned to a single π MO (HOMO-1) that corresponds to HOMO of other Pc molecules [2]. DFT-MO calculation suggests that the HOMO band of the MnPc is related to Mn-3d-derived state. However, we are in progress to conclude the assignment which character of 3d MOs is responsible to this state because of a variety in the spin configuration.

Figure 1(b) shows the observed θ dependences of HOMO and HOMO-1 intensities obtained at hv =20eV. Both patterns show a similar distribution to give a maximum around $\theta=50^{o}$, though the intensity is slightly different around $\theta=25^{o}$. Figure 1(c) shows the θ dependences of HOMO and HOMO-1 intensities at hv =28eV. The patterns are different significantly between HOMO and HOMO-1. The intensity shows maximum at $\theta=8^{o}$ for the HOMO and $\theta=30^{o}$ for the HOMO-1. The difference in the θ distributions might be related to the different orbital distribution, that is, 3d-orbital for HOMO and 2p-orbital for HOMO-1.

Now we are trying to simulate the patterns by taking into account the characteristics of 3d-orbitals with theoretical calculations, multiple-scattering approximation combined with MO calculation [1]. ARUPS results would be helpful for making assignments of complex electronic structure such as a mixed valence and spin configuration of organometalic compounds.

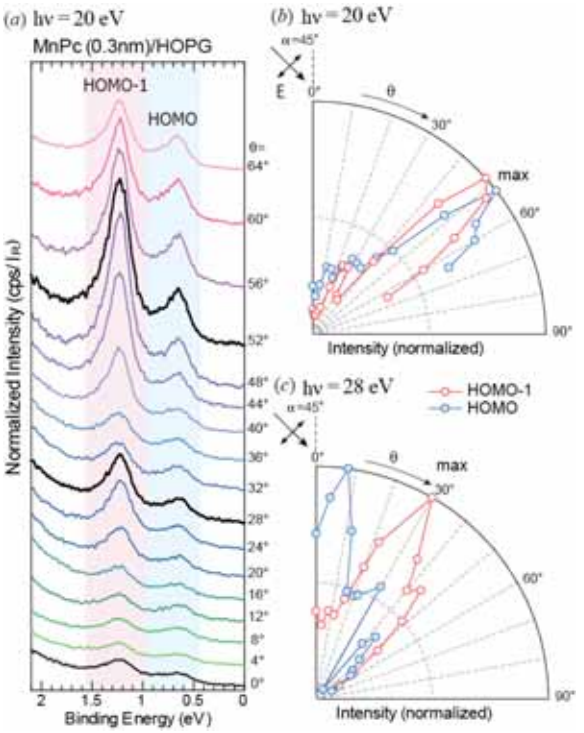

Fig. 1.(a) θ dependence of ARUPS of 1-ML(0.3nm) MnPc on HOPG measured at hv=20eV. Observed θ patterns of the HOMO band (blue circles) and HOMO-1 band (red circles) obtained by hv=20 eV (b) and hv=28eV (c).

[1] S. Nagamatsu et al, e-J. Surf. Sci. Nanotech. **3** (2005) 461.
[2] H. Fukagawa et al, Phys. Rev. B **73** (2005) 041302(R).
[#]Present add: Graduate School of Advanced Integration Science, Chiba University

BL8B2

Electronic Structure of Lithium Phthalocyanine Thin Film

S. Tanaka[1, 2], K. Watanabe[3], Y. Yoshida[3], I. Hiromitsu[3], K. Yoshino[2]
[1] *Center of Integrated Research in Science, Shimane University, Matsue 690-8504 Japan*
[2] *Research Project Promotion Institute, Shimane University, Matsue 690-8504 Japan*
[3] *Faculty of Science and Engineering, Shimane University, Matsue 690-8504 Japan*

Introduction

Phthalocyanine (Pc) and metal phthalocyanines have attracted much interest for their semiconducting properties implying many interesting applications including photovoltaics, photoconductors and sensors. Lithium phthalocyanine (LiPc) is known as a stable neutral radical and is one of a few intrinsic semiconducting molecules [1, 2]. The chemical structure of LiPc is shown in Fig. 1. It is known that LiPc has rather high conductivity and a peculiar UV-VIS absorption spectrum as compared to other metal phthalocyanines such as ZnPc, CuPc or TiOPc. Thus, the structures of LiPc and those properties are interesting, and these have been the subject of many studies [2-4]. In this work, we investigate the electronic structures of thin films of LiPc on an Au substrate. The energy level alignment at the LiPc/Au interface is revealed from the photoelectron spectra as a function of the LiPc thickness.

Experimental

LiPc was synthesized by electrochemical oxidation of dilithium phthalocyanine (Li_2Pc) following the synthesis procedure described in literatures [1]. The purification of LiPc was done by vacuum sublimation. LiPc was deposited on an Au substrate. Evaporation of LiPc was performed using a glass-cell evaporator after careful outgassing, keeping the pressure of the preparation chamber at less than 4×10^{-6} Pa. All the photoelectron measurements were carried out at photon incident angle of 45°, $h\nu = 40$ eV, and sample temperature of about 295 K. Photoelectron spectra of metal-free phthalocyanine (H_2Pc) were also measured for comparison.

Results and Discussion

Figure 2 shows the photoelectron spectra of LiPc grown on Au as a function of thickness. The abscissa is the binding energy relative to the Fermi energy of Au. The energy difference between the HOMO of LiPc and Fermi level of Au at the interface is about 0.3 eV. This suggests that the energy barrier height for hole injection from Au to LiPc is relatively small. From the secondary electron cutoff, it was observed that the energy of the vacuum level sharply decreases by about 0.4 eV within the thin-layer region up to around 1 nm (not shown here). The abrupt lowering of vacuum level at metal/organic interfaces is ascribed to the formation of the interface dipole [5]. The downward of the vacuum level caused by the LiPc deposition suggests the formation of interfacial dipole layer with LiPc side positively charged. In the thick-layer region (10 – 30 nm), no obvious shift was observed at the HOMO peak and the secondary electron cutoff. These results indicate that the thermal equilibrium condition of the LiPc layer is achieved in the thin-layer region (~ 10nm).

The HOMO peak of LiPc appears at around 1.1 eV. The binding energy and the intensity of the LiPc HOMO peak were smaller than those of the H_2Pc HOMO peak. The ionization potential of the LiPc thin film and that of the H_2Pc thin film were estimated at about 5.1 eV and 5.2 eV, respectively, from the secondary cutoff and the lower cutoff of the HOMO peak. The HOMO peak intensity of LiPc was smaller than that of H_2Pc, reflecting a characteristic of the unpaired electron of LiPc.

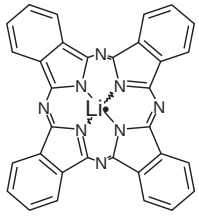

Fig. 1 Chemical structure of lithium phthalocyanince.

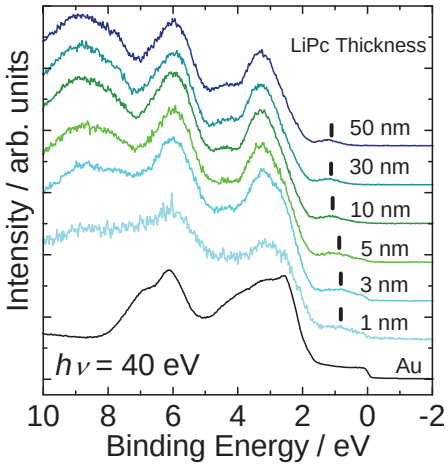

Fig. 2 Photoelectron spectra of LiPc film incrementally deposited on Au.

[1] P. Turek *et al.*, Chem. Phys. Lett. **134** (1987) 471.
[2] M. Brinkmann *et al.*, Thin Solid FIms **324** (1998) 68.
[3] T. Kimura *et al.*, Chem. Phys. **253** (2000) 125.
[4] N. Sato *et al.*, Appl. Surf. Sci. **212-213** (2003) 438.
[5] H. Ishii *et al.*, Adv. Mat. **11** (1999) 605.

BL8B2

Structural Change in Lithium Phthalocyanine/Poly(3-hexylthiopehne) Interface Caused by Annealing

S. Tanaka[1, 2], K. Watanabe[3], Y. Yoshida[3], I. Hiromitsu[3], K. Yoshino[2]

[1] *Center of Integrated Research in Science, Shimane University, Matsue 690-8504 Japan*

[2] *Research Project Promotion Institute, Shimane University, Matsue 690-8504 Japan*

[3] *Faculty of Science and Engineering, Shimane University, Matsue 690-8504 Japan*

Introduction

The conjugated polymers are promising material for organic semiconductor devices. Poly (3-hexyl -thiophene) (P3HT) is one of π–conjugated polymers. P3HT is used widely in polymer field-effect transistors, photovoltaic cells, and light-emitting diodes because of its characteristic properties such as solubility for various organic solvents, fusibility at relatively low temperature, and relatively high carrier mobilities. [1] The control of electrical properties in the conjugated polymers is a major issue for further device applications. Doping is the one way to control the electric property of the conjugated polymers.

We have recently studied an effective molecular doping for the P3HT film. Lithium phthalocyanine (LiPc) molecule is a candidate of the molecular dopant for P3HT. In this work we measured the variation of the photoelectron spectra of the P3HT films caused by annealing following a deposition of LiPc molecules.

Experimental

The molecular structure of P3HT and LiPc are shown in Fig. 1. The P3HT sample was prepared with a chloroform solution of P3HT casting on a clean Au foil. The sample was immediately introduced into the vacuum chamber. The annealing of the sample was done in the preparation chamber *in situ*.

Results and Discussion

Figure 2 shows the photoelectron spectra of (a) P3HT, (b) LiPc (3nm) on P3HT, and (c) LiPc (3nm) on P3HT after annealing at 373 K. The abscissa is the binding energy relative to the Fermi energy of Au. It is expected from the shape of the spectrum that the P3HT sample was slightly charging because of the thickness of the P3HT film. In the P3HT spectrum, the intense feature extending from 12 to 5 eV contains the levels associated to the alkyl groups and the π-electrons of the thiophene rings contributes to the region below 5 eV [3]. The LiPc layer with 3 nm thickness was deposited on to the P3HT layer by vacuum evaporation, and the photoelectron spectrum (Fig. 2. (b)) was measured *in situ*. The feature of the photoelectron spectrum showed the electronic structure almost only of LiPc; hence, the surface of the P3HT layer was fully covered with the LiPc molecules. After the measurement of the photoelectron spectrum, the sample of LiPc (3 nm) on P3HT was annealed at 373 K (100 min) *in situ*. The spectrum of fig. 2 (c) is the photoelectron spectrum after the annealing. As seen in fig. 2 (c), the spectrum showed not the LiPc electronic structures but the P3HT electronic structures. Because of the surface sensitivity of the photoelectron spectroscopy, these results indicate that there were few LiPc molecules on the sample surface after annealing. A possible reason of the drastic change caused by annealing is that the LiPc molecules were diffused into the P3HT layer with the conformation change by the annealing. The Li 1s spectra showed peak shift and the splitting caused by annealing (not shown). To investigate the relations between the doping mechanism and the variations of the photoelectron spectra, further studies are now in progress.

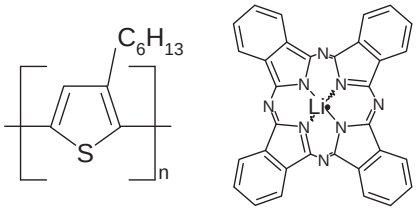

Fig. 1 Chemical structures of (a) poly(3-hexyl -thiophene) and (b) lithium phthalocyanince.

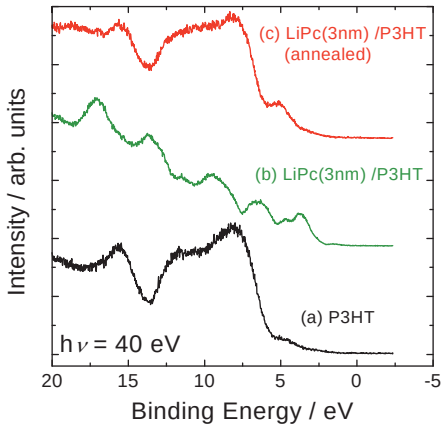

Fig. 2. The photoemission spectra of (a) P3HT, (b) LiPc (3 nm) on P3HT, and (c) LiPc (3 nm) on P3HT after annealing at 373 K.

[1] K. Yoshino, M. Onoda, Polymer Electronics, Corona, Tokyo, (1996) (in Japanese).

[2] M. Brinkmann *et al.*, Thin Solid Films **324** (1998) 68.

[3] R. Lazzaroni *et al.*, J. Chem. Phys. **93** (1990) 4433.

BL8B2

Electronic Structure of Singlet Biradical Hydrocarbon Ph_2-IDPL Thin Film

K. Kaname, T. Kubo[1], H. Yamane[2], R. Sumii, K. Nakasuji[3], Y. Morita[1], K. Seki[2,4]

Research Center for Materials Science, Nagoya University, Furo-cho, Chikusaku Nagoya 464-8602 Japan

[1]Department of Chemistry, Graduate School of Science, Osaka University, Machikaneyama 1-1, Toyonaka, Osaka 560-0043, Japan

[2]Department of Chemistry, Graduate School of Science, Nagoya University, Furo-cho, Chikusa-ku, Nagoya 464-8602, Japan

[3] Fukui University of Technology, Gakuen 3-6-1, Fukui-shi, Fukui 910-0028, Japan

[4] Institute for Advanced Research, Nagoya University, Furo-cho, Chikusa-ku, Nagoya 464-8602, Japan

Realization of the columnar stackings of planar molecule on the substrate by intermolecular interaction between extended π-systems is widely interested matter in surface physics and organic device technology. Diphenyl derivative of s-indacenodiphenalene (Ph_2-IDPL) was isolated and characterized as a singlet biradical hydrocarbon by T. Kubo *et al* [1]. Ph_2-IDPL was reported to have strong intra- and intermolecular interaction leading to π- π stacking distance (3.137 Å) for the crystal, which is substantially shorter than the van der Waals contact of carbon atoms (3.4 Å). In Ph_2-IDPL crystal, staggered stacking of the molecules forms ideal one-dimensional molecular chain. Such strong intermolecular interaction in the ground state of Ph_2-IDPL molecule is caused from the interaction between unpaired electrons characteristic of biradical molecule. It is expected that tendency of Ph_2-IDPL molecules to undergo facile self-association on the substrate and form highly oriented film with π- π stacking originated form the strong intermolecular interaction.

In this report, the electronic structure of Ph_2-IDPL film deposited on single crystal GeS(100) surgface were investigated by angle-resolved ultraviolet photoemission spectroscopy (ARUPS).

ARUPS measurements were performed in UVSOR BL-8B2. Base pressure of the experimental chamber was under 5×10^{-8} Pa. Clean surface of GeS substrate was obtained by cleaving the surface in vacuum. Thickness of the Ph_2-IDPL film was monitored by quartz microbalance.

Figure 1 shows UPS spectra of Ph_2-IDPL film with the thickness of 0.4 nm on GeS(100) surface. θ stands for take-off angle of photoelectron. Dependence of the spectral shape on θ was clearly observed. Based on ARUPS measurements as shown in Fig. 1 the momentum $k_{//}$ dependences of the energy of each spectral features labeled A, B, C, D and E are presented in Fig. 2. Those features show clear energy dispersion characteristic of one-dimensional system, which indicates the formation of well-ordered Ph_2-IDPL film with anisotropy on GeS(100) surface. Such one-dimensional energy dispersion was predicted in the framework of extended Hueckel (EH) theory [1]. Especially, the behaviors of A and B are qualitatively well explained by the energy band calculation by using EH theory. However, observed energy width of the dispersion (*e.g.* about 0.1 eV and 0.5 eV for A and B, respectively) is smaller than that estimated by energy band calculation [1].

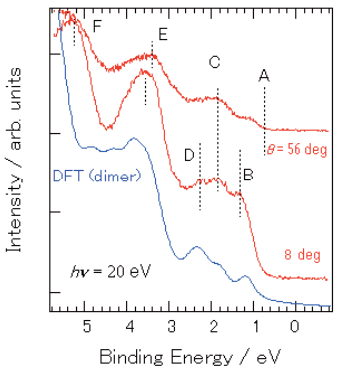

Fig. 1 UPS spectra of Ph_2-IDPL film on GeS(100) surface. The normal emission is origin of θ.

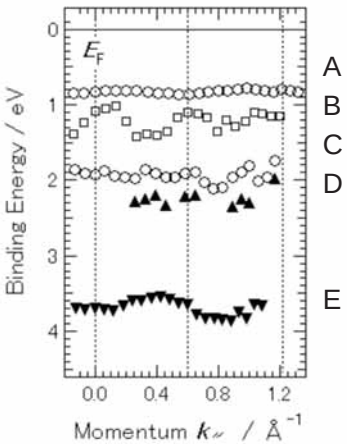

Fig. 2 Momentum dependence of the energy of the spectral features labeled in Fig. 1. Dotted vertical bars represents the boundary of Brillouin zone calculated by lattice constant along the molecular stacking in crystal.

[1] T. Kubo, K. Nakasuji *et al.*, Angew. Chem. Int. Ed., 44 6564 (2005).

BL8B2

Ultraviolet Photoelectron Spectra of $(YC)_2@C_{82}$ and $Y_2@C_{82}$*

S. Hino [1†], N. Wanita[1], K. Iwasaki[1], D. Yoshimura[2,3], T. Akachi[4],
T. Inoue[4], Y. Ito[4], T. Sugai[4], H. Shinohara[4]

[1] *Chiba University, Inage-ku, Chiba 263-8522 Japan*
[2] *Institute for Molecular Science, Okazaki 444-8585 Japan*
[3] *Research Center of Material Science, Nagoya University, Nagoya 464-8602 Japan*
[4] *Faculty of Science, Nagoya University, Nagoya 464-8602* Japan

Recently, encapsulation of multiple atoms, such as metal clusters [1, 2], metal nitrides [3] and metal –carbon clusters [4] inside the cage has been reported. These metallofullerenes are considered a different class from mono-metal atom encapsulated metallofullerenes from the view point of electron transfer from the encapsulated atoms to the fullerene cage. This is thought to be because encapsulated atoms may form chemical bonds among them as well as they may form bonds to the carbon atoms that constitute the cage.

Recently, numerous yttrium and carbon atoms encapsulated metallofullerenes ($(YC)_2@C_{82}$) have been reported, and three isomers were isolated [4]. Yttrium atoms have also been reported to be encapsulated into the fullerene cage, and three $Y_2@C_{82}$ isomers were identified [4]. NMR spectra of a $(YC)_2@C_{82}$ (III) isomer [4] and $Y_2@C_{82}$(III) revealed that their cage structures are exactly the same and, their absorption spectra resemble each other, suggesting their analogous electronic structures.

Figure 2 shows the UPS of $(YC)_2@C_{82}$ (III). The intensity of each structure in the UPS of $Y_2@C_{82}$ (III) labeled A – I changes upon tuning the incident photon energy, which is typical spectroscopic behavior of fullerenes. The USP of $(YC)_2@C_{82}$ (III) resemble those of $Y_2@C_{82}$ (III). To clarify the difference between these two metallofullerenes, their UPS obtained with 30 eV photon are shown in Fig.2

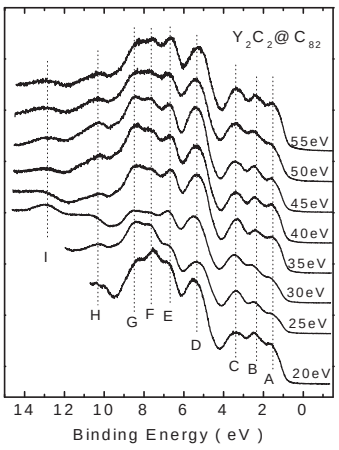

Fig. 1 Incident photon energy dependence of the UPS of $(YC)_2@C_{82}$ (I).

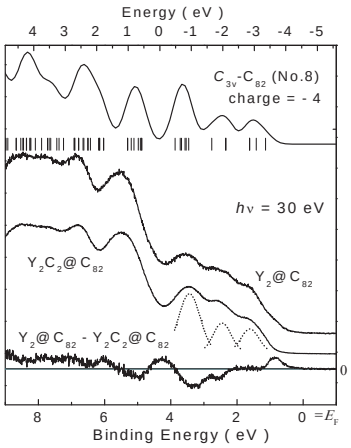

Fig.2 Comparison of the UPS of $(YC)_2@C_{82}$ and $Y_2@C_{82}$ isomers. Difference spectrum between them (bottom) and simulation spectra (top) obtained by MO calculation.

The first three structures of $(YC)_2@C_{82}$ (III) can be deconvoluted into three components with intensity ratio of 4 : 5 : 9. This is well reproduced by a simulation spectrum (top in Fig. 2) calculated using geometry of C_{3v}-C_{82} (No.5) [5] with additional 4 electrons on the cage. This finding indicates $(YC)^{2+}{}_2@C_{82}{}^{4-}$ is the plausible oxidation state.

Onset energy of $Y_2@C_{82}$ (III) is slightly smaller than that of $(YC)_2@C_{82}$ (III). Difference spectrum between them (bottom in Fig. 2) reveals two additional electrons on $Y_2@C_{82}$ (III). Thus, the oxidation state of this metallofullerene might be $Y^{3+}{}_2@C_{82}{}^{6-}$. Since the oxidation state of Y must be + 3, probably two electrons in $(YC)_2@C_{82}$ (III) might be used either to form the bonds between Y and C or to donate electrons to acetylide.

* This work was published in Phys. Rev. B **72** (2005) 195424.

† present address, Ehime University, Matsuyama, Ehime 790-8577.

[1] M. Takata *et al*., Phys. Rev Lett. **83** (1999) 2214.
[2] C.-R. Wang *et al*., Nature **408** (2000) 426.
[3] S. Stevenson *et al. ibid*. (1999) 55.
[4] T. Inoue *et al*., Chem. Phys. Lett. **382** (2003) 226 and J. Phys. Chem. B **108** (2004) 7573.
[5] P. W. Fowler, "An atlas of Fullerenes", Oxford Press, Oxford, 1995.

BL8B2

Ultraviolet Photoelectron Spectra of Three Tm@C_{82} Isomers*

S.Hino [1†], N. Wanita[1], K. Iwsaki [1], D. Yoshimura[2,3], N. Ozawa[4],

T. Kodama[4], K. Sakaguchi[4], H. Nishikawa[4], I. Ikemoto[4], K. Kikuchi[4]

[1]*Chiba University, Inage-ku, Chiba 263-8522 Japan*
[2]*Institute for Molecular Science, Okazaki 444-8585 Japan*
[3]*Research Center of Material Science, Nagoya University, Nagoya 464-8602 Japan*
[4]*Faculty of Science, Tokyo Metropolitan University, Hachioji, Tokyo 192-0397* Japan

Up to now a lot of metallofullerenes have been synthesized [1] and among them the most abundantly obtainable metallofullerene seem to have C_{82} cage. There are nine isolated pentagon rule (IPR) satisfying cage structures for C_{82}. While it seems that trivalent metal atom accommodates only in C_{2v} and C_s cages, divalent metal atoms prefer more cages. Tm atom is entrapped inside the C_{82} cage and three Tm@C_{82} isomers have been reported [2, 3]. We present the UPS of three Tm@C_{82} isomers and compare them with previously reported one [4] and those of two Ca@C_{82} isomers [5] and discuss the correspondence among these metallofullerenes. Cage structures of three Tm@C_{82} isomers are also proposed with an aid of molecular orbital calculation.

Figure 1 shows the valence band UPS one of three Tm@C_{82} isomers, isomer (I) obtained with hν = 20 – 55 eV photon energy. Spectral onsets of three isomers are 0.85 eV (I), 0.75 eV (II) and 0.9 eV (III). The onset energies of Tm@C_{82} isomers are relatively large compared with those of La@C_{82} and Gd@C_{82} but almost the same as those of Ca@C_{82} isomers [4].

Figure 2 shows the UPS of three Tm@C_{82} isomers and two Ca@C_{82} isomers. The UPS of Tm@C_{82} (II) and Ca@C_{82} (III) are essentially the same which indicates that these two metallofullerenes have the same electronic structure derived from the same cage structure. The UPS and MO calculation proposed C_2(c) cage structure for the geometry of Ca@C_{82} (III) [6] and this deduction was later supported by the NMR measurements [7]. Further the NMR on Tm@C_{82} (II) predicts the same C_2 symmetry. On the other hand,

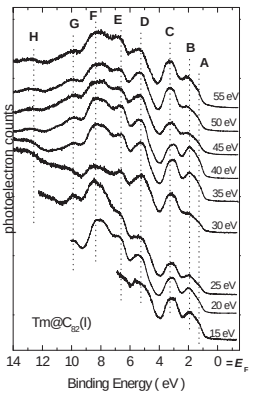

Fig. 1 Incident photon energy dependence of the UPS of Tm@C_{82} (I).

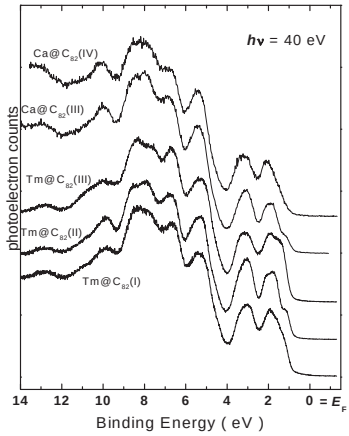

Fig.2 Comparison of the UPS of two Ca@C_{82} isomers and three Tm@C_{82} isomers.

these spectra correspond with the HeI and HeII excited spectra reported by Pichler's group who claimed that they measured C_{3v}-Tm@C_{82} [4]. That is, the metallofullerenes that we and Pichler's group have measured are the identically the same species and Pichler's claim of symmetry definition was wrong.

The UPS of three Tm@C_{82} isomers were compared with MO calculation and it was found that their cage structures are C_s(c) cage structure for Tm@C_{82} (I), C_2(c) for Tm@C_{82} (II) and C_{2v} for Tm@C_{82} (III)

* This work was published in Chem. Phys. Lett. **402**, 217 (2005).

† present address : Ehime University, Matsuyama, Ehime 790-8577 Japan

[1] for example, H. Shinohara, Rep. Prog. Phys. **63** (2000) 843.
[2] U. Kirbachet al., Chem. Int. Ed. Engl. **35** (1996) 2380.
[3] T. Kodama et al., J. Ame. Chem. Soc. **124** (2002) 1452.
[4] T. Pichler et al., Appl. Phys. A**66** (1998) 281
[5] S. Hino et al., Chem. Phys. Lett. **230** (1994) 165.
[6] S. Hino et al., Chem. Phys. Letts. **227** (2001) 65.
[7] T. Kodama et al., Chem. Phys. Letts. **377** (2003) 197.

BL8B2

Electronic Structure at Highly Ordered Pentacene/Cu(110) Interface: Energy-Level Splitting and Energy-Band Dispersion

H. Yamane [1], E. Kawabe [1], R. Sumii [2], K. Kanai [2], Y. Ouchi [1], K. Seki [1,2]
[1] *Department of Chemistry, Nagoya University, Nagoya 464-8402 Japan*
[2] *Research Center for Materials Science, Nagoya University, Nagoya 464-8602 Japan*

Introduction

The electronic structure at organic/metal interfaces, in particular the energy positions of the highest-occupied and lowest-unoccupied molecular orbital (HOMO and LUMO) levels relative to the Fermi level (E_F) of metal electrodes, plays a crucial role in determining the charge injection barrier in (opto) electronic devices using organic semiconductors. Therefore it is natural that many research groups have been investigating the energy-level alignment at organic-related interfaces in order to elucidate the energetics at the interfaces. For deeper understanding of the energetics at organic/metal interfaces, a more pertinent experimental approach to this issue would be the use a well-characterized system in quantitative electron spectroscopic measurements. In this work, we studied the electronic structure of highly-ordered monolayer of pentacene prepared on Cu(110) surface by angle-resolved UV photoemission spectroscopy (ARUPS) using synchrotron radiation. We observed a distinctive electronic structure at the interface, which is completely different from those of the gas- and bulk-phase pentacene.

Experimental

The purified pentacene was carefully evaporated onto the clean Cu(110) surfaces, which was kept at 500 K during the deposition.

The azimuthal angle (ϕ) dependence of ARUPS spectra was measured at the photon energy ($h\nu$) of 20 eV, the photon incidence angle (α) of 60°, take-off angle (θ) of 58° from the surface normal, and the temperature of 300 K. The origin of the azimuthal angle ϕ = 0° was defined so that the electric-field vector of the incident photon is on the incident plane containing the substrate [1-10] direction and the surface normal.

Results and Discussion

The ϕ dependences of the ARUPS spectra with a step of 3° for the clean Cu(110) substrate and the pentacene monolayer on the Cu(110) substrate are shown in Fig. 1. The abscissa is binding energy (E_b) relative to the substrate E_F, and the spectra are normalized to the incident photon flux. As a reference, we also show the UPS spectrum of the gas-phase pentacene [1], which is shifted to align the lowest-E_b peak to that of the pentacene monolayer on Cu(110) at ϕ = 0°. For the Cu(110) substrate, the peak S due to the direct s,p-band transition appears at 1.9 eV when ϕ = 0° and gradually shifts toward the low-E_b side until ϕ reaches 30°. Upon formation of the pentacene monolayer on the substrate, the intensity of this substrate peak S decreases, and the new peaks A, B, and C appear with the continuous change in the peak positions with ϕ. We note that the separation between A and B is about 0.7 eV, while the E_b difference between the HOMO and HOMO-1 peaks in the gas-phase spectrum is much larger (1.4 eV) [1]. This discrepancy is in contrast to the case of the physisorbed pentacene monolayer on highly oriented pyrolytic graphite, where the relative energies of the peaks correspond well with those in the gas phase [2]. Thus we can consider that the peaks A and B are formed by the strong molecule-substrate interaction.

From the consideration of symmetry selection rules and the θ dependences of the ARUPS spectra [3], we can deduce that (i) the peaks A and B originate from the energy-level splitting of the original HOMO level and that (ii) the continuous change in the peak position with ϕ originates from the intermolecular energy-band dispersion. In this system, the intermolecular interaction via direct contact is considerably weak, and these findings may originate from the intermolecular interaction via the substrate due to the significant hybridization of the MOs and the substrate.

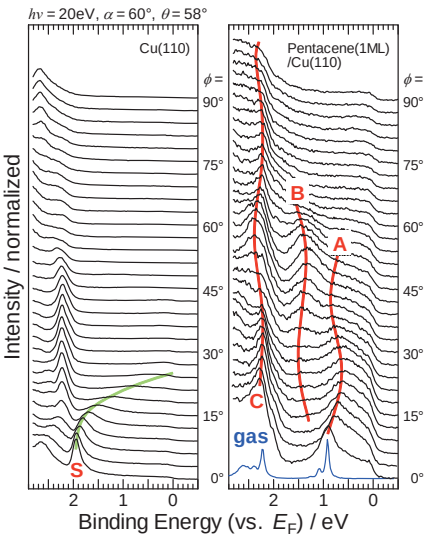

Fig. 1 Azimuthal angle (ϕ) dependence of the ARUPS spectra for the Cu(110) substrate (left) and the pentacene monolayer on Cu(110) (right).

[1] V. Coropceanu *et al.*, Phys. Rev. Lett. **89**, (2002) 275503.
[2] H. Yamane *et al.*, Phys. Rev. B **72** (2005) 153412.
[3] H. Yamane *et al.*, UVSOR Activity Report 2005 (2006) 113.